AD-A169 332 PROPAGATION OF SIGNALS IN THE FREQUENCY BAND BETWEEN 30 MHZ AND 100 MHZ(U) NAVAL OCEAN SYSTEMS CENTER SAN DIEGO CA W POWERS ET AL. SEP 85 NOSC/TR-1087 1/2

UNCLASSIFIED F/G 20/14 NL

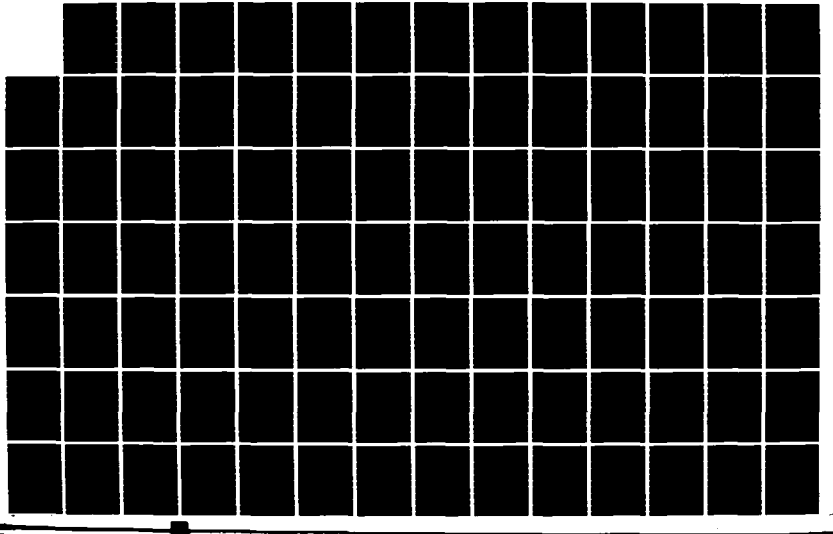

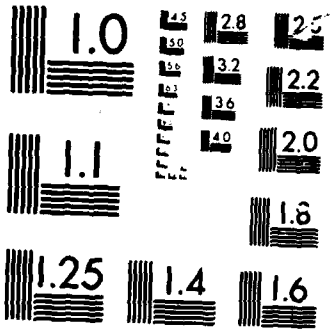

(12)

TR 1087

Technical Report 1087
15 September 1985

PROPAGATION OF SIGNALS IN THE FREQUENCY BAND BETWEEN 30 MHz AND 100 MHz

W. Powers
R. B. Rose

Naval Ocean Systems Center
San Diego, California 92152

NAVAL OCEAN SYSTEMS CENTER

San Diego, California 92152-5000

F. M. PESTORIUS, CAPT, USN
Commander

R. M. HILLYER
Technical Director

ADMINISTRATIVE INFORMATION

This task was performed for the Signal Intelligence Support Module program as part of the Joint Tactical Fusion Program (ARMY) under program element RDA, DA (NOSC Project SY32). The work is a cooperative effort performed by the Signal Exploitation Branch (Code 772) and the Ionospheric Branch, Code 544 of the Naval Ocean Systems Center, San Diego, CA 92152-5000 and reflects work performed between 1 October 1984 and 30 September 1985.

Released by
R.B. Rose, Head
Signals Exploitation Branch

Under authority of
R.L. Brandenburg, Head (Acting)
Signals Warfare Division

AS

UNCLASSIFIED
SECURITY CLASSIFICATION OF THIS PAGE

REPORT DOCUMENTATION PAGE

1a REPORT SECURITY CLASSIFICATION UNCLASSIFIED	1b RESTRICTIVE MARKINGS
2a SECURITY CLASSIFICATION AUTHORITY	3 DISTRIBUTION/AVAILABILITY OF REPORT Approved for public release; distribution is unlimited.
2b DECLASSIFICATION/DOWNGRADING SCHEDULE	
4 PERFORMING ORGANIZATION REPORT NUMBER(S) NOSC TR 1087	5 MONITORING ORGANIZATION REPORT NUMBER(S)
6a NAME OF PERFORMING ORGANIZATION Naval Ocean Systems Center 6b OFFICE SYMBOL (if applicable) Code 772	7a NAME OF MONITORING ORGANIZATION
6c ADDRESS (City, State and ZIP Code) San Diego, CA 92152-5000	7b ADDRESS (City, State and ZIP Code)
8a NAME OF FUNDING/SPONSORING ORGANIZATION U.S. Army, Joint Tactical Fusion Program 8b OFFICE SYMBOL (if applicable) ARMY-NA	9 PROCUREMENT INSTRUMENT IDENTIFICATION NUMBER
8c ADDRESS (City, State and ZIP Code) McLean, VA 22102	10 SOURCE OF FUNDING NUMBERS PROGRAM ELEMENT NO: RDA PROJECT NO: ARMY TASK NO: 750-SY32 Agency Accession: DN305 116

11 TITLE (Include Security Classification)

Propagation of Signals in the Frequency Band Between 30 MHz and 100 MHz

12 PERSONAL AUTHOR(S)
W. Powers, R.B. Rose

13a TYPE OF REPORT	13b TIME COVERED	14 DATE OF REPORT (Year, Month, Day)	15 PAGE COUNT
Final	FROM Oct 84 TO Sep 85	September 1985	97

16 SUPPLEMENTARY NOTATION

17 COSATI CODES			18 SUBJECT TERMS (Continue on reverse if necessary and identify by block number)
FIELD	GROUP	SUB GROUP	LoVHF propagation, near-surface propagation, transmission models

19 ABSTRACT (Continue on reverse if necessary and identify by block number)

The current state of knowledge of propagation phenomena at radio frequencies between 30 and 100 MHz is reviewed. The ability to perform signal coverage calculation for the various modes of propagation is assessed and appropriate formulation presented. The groundwork for a continuation modeling program is established.

20 DISTRIBUTION/AVAILABILITY OF ABSTRACT	21 ABSTRACT SECURITY CLASSIFICATION	
☒ UNCLASSIFIED/UNLIMITED ☐ SAME AS RPT ☐ DTIC USERS	UNCLASSIFIED	
22a NAME OF RESPONSIBLE INDIVIDUAL R. B. Rose	22b TELEPHONE (Include Area Code) (619) 225-2924	22c OFFICE SYMBOL Code 772

DD FORM 1473, 84 JAN

83 APR EDITION MAY BE USED UNTIL EXHAUSTED
ALL OTHER EDITIONS ARE OBSOLETE

UNCLASSIFIED
SECURITY CLASSIFICATION OF THIS PAGE

CONTENTS

1. INTRODUCTION

Propagation in the LoVHF (30-100 MHz) frequency band possesses characteristics common to both HF (3-30 MHz) and HiVHF (100-300 MHz) propagation. It is this feature which makes this frequency band both interesting and complex.

The primary interest of this report is the modes of propagation between surface- or near-surface-based transmitters and receivers. For a given range, the strength, geographical and temporal dependence, and likelihood of a particular mode of propagation will be discussed. In the last section, various existing models that could be used to describe the field strength and transmission loss in the LoVHF band are assessed. These models and the discussion of the various modes of propagation fall roughly into two groups: (i) those that affect ranges less than 500 km and (ii) those that affect ranges greater than 500 km.

2. RANGES LESS THAN 500 km

The line-of-sight distance of transmission in the 30-100 MHz band is dependent on the degree to which the neutral atmosphere near the surface of the earth refracts the rays. Under normal conditions the index of refraction decreases as the radial distance from the center of the earth increases. The ray is bent back toward the earth, but because its curvature is less than that of the earth's, it does not return to the earth's surface. However, under certain meteorological conditions the atmosphere will bend the ray less than under normal conditions; in other cases, it will bend it more. In the former case, the atmosphere is referred to as subrefractive; in the latter case, as superrefractive. For an index of refraction n, which is approximately linear near the surface of the earth, these effects can be approximately taken into

account by defining an effective radius of the earth R_e. In this case we obtain for the line-of-sight distance d_{los} (Reed and Russell, 1966)

$$d_{los} = (2R_e)^{\frac{1}{2}}(\sqrt{h_1} + \sqrt{h_2}) \ , \tag{1a}$$

where

$$R_e = \frac{\alpha}{1 + \alpha \ dn/dh} \ . \tag{1b}$$

Here, h_1 and h_2 are the heights of the receiving and transmitting antennas, dn/dh is the first derivative of the index of refraction with respect to height above the surface of the earth, and α is the radius of the earth.

For simplicity we will assume that, within the line-of-sight distance, the radiation from the transmitter to the receiver is not obstructed by objects much larger than a wavelength. In this case, for distances less than or similar to d_{los} and for distances much greater than a wavelength from the transmitter, the signal strength at the transmitter is due principally to the contributions from the direct ray and the ray which is reflected from the earth's surface (Freehafer, 1964). As the elevation angle of the reflected ray approaches zero, the contribution from the surface wave must be taken into account (Reed and Russell, 1966). This is especially true over seawater (Reed and Russell, 1966).

There is a region in which the geometrical optics field and the diffracted field interfere. This region is referred to as the intermediate region (Kerr, 1964). For still larger ranges beyond the radio horizon, the diffracted field becomes the primary contribution. For ranges greater than about 50 km beyond the radio horizon, the received field decays less rapidly than that predicted by the diffracted field alone (Reed and Russell, 1966). At these ranges, scattering from irregularities in the troposphere contributes

to the received field. The signal propagated by means of tropospheric scattering is about 100 dB below that of free space at a distance of about 650 km, and as the range decreases, it increases at a rate of approximately 1/4 of a dB/km (Reed and Russell, 1966). The received power falls at a rate of between $1/d^7$ for broadbeam antennas and $1/d^9$ for narrowbeam antennas (Wheelon, 1959), where d is the distance between the transmitter and receiver. The wavelength dependence of the received power varies as λ for broadbeam antennas and as λ^3 for narrowbeam antennas (Wheelon, 1959). The signal strengths follow a seasonal pattern, being stronger in the summer than in the winter (Dolukhanov, 1971). This is apparently due to the fact that in the summer the rate at which the refractive index decreases with height increases. This effect results in larger bending of the rays, smaller angle scattering, and larger fluctuations in the dielectric constant (Dolukhanov, 1971). The net effect of these differences is to produce a larger scattered field.

Because narrowbeam antennas limit the spread in arrival time, the frequency coherence of the received field is improved (Booker and DeBettencourt, 1955). The larger the distance between transmitter and receiver, the greater the spread in arrival times and the more rapid the rate of frequency fading (Booker and DeBettencourt, 1955). Typically, time delays are on the order of tenths of microseconds for beyond-the-horizon paths (Schwartz, Bennett and Stein, 1966). This implies a correlation bandwidth from hundreds of kilohertz to a few megahertz (Stein and Jones, 1967). Because the tropospheric scattering region is in constant motion, the scattered signal is both Doppler shifted and spread. Apparently the Doppler shift is generally very small. The fading rate is proportional to frequency, with fading rates less than 1 Hz in the LoVHF band (Hall, 1979, Schwartz, Bennett and Stein, 1966).

2.1 DUCTING

Under superrefractive conditions, the curvature of a ray can exceed that of the earth, and the possibility exists for the creation of a ground-based duct. Under these circumstances, it is possible for the ray, by series of hops between the reflection level and the earth, to propagate well beyond the radio horizon. However, in order to obey boundary conditions at the earth's surface, only a certain discrete set of modes is permitted (Budden, 1961a). The maximum height at which a particular mode is reflected corresponds closely to the height associated with the minimum value of the index of refraction. This height defines the thickness of the duct which guides the energy around the earth. If the duct thickness is too small, the duct will be very leaky and its ability to guide the energy greatly reduced. For a given duct thickness, the higher the frequency of propagation, the less leaky the duct. For sufficiently thick ducts, field strengths on the order of their free space value and greater can be propagated over hundreds and possibly thousands of kilometers (Hitney et al., 1985, Pappert and Goodhart, 1977, Vergara et al., 1962). However, the elevation angles of the modes which are trapped by tropospheric ducts are typically below 1 deg (Bean and Dutton, 1966); hence, the ability of a transmitter to couple energy into these ducts is critically dependent upon the power transmitted at very low elevation angles (Vergara et al., 1962). Even when the duct thickness is insufficient to trap the wave, partial reflection still returns energy to the earth's surface. As a consequence, the signal can often be as much as 10 dB greater than that expected by diffraction alone (Pappert and Goodhart, 1979, Vergara et al., 1962).

The refractivity N is defined by $N = (n - 1)10^6$, where n is the index of refraction. In practical applications N can be related to the pressure P in

millibars, the temperature T in degrees Kelvin, and the partial pressure of water vapor e by the expression

$$N = \frac{77.6}{T}\left[P + \frac{4810e}{T}\right] \qquad (2)$$

Normally, the temperature and humidity decrease with increasing height above the earth's surface in such a way that the refractivity decreases with height (Bean and Dutton, 1966). Ducts are generally produced by a greater than average rate of decrease of vapor pressure, a less than average rate of decrease of temperature, or both. There are three distinct classes of ducts: evaporation ducts, surface-based ducts, and elevated ducts (Hitney et al., 1985). Evaporation ducts are produced near the surface of the ocean by the rapidly changing humidity of the air. They are almost always present and are generally less than 40 m thick (Hitney et al., 1985). Surface-based ducts are generally produced by the motion of large masses of air into a region having different meteorological properties (Bean and Dutton, 1966). In a typical strong ducting situation, dry, warm air will move in over a cold ocean, thus producing not only a rapid decrease in vapor pressure, but a temperature inversion. The base of a surface-based duct is located at ground level. Its top can be as high as several hundred meters above the earth's surface (Hitney et al., 1985). Elevated ducts are formed by processes similar to those which form surface-based ducts; however, the base of the duct is not located at ground level. Evaporation ducts are generally too thin to support LoVHF propagation; however, surface-based ducts can be an important feature of LoVHF propagation (Hitney et al., 1985). Elevated ducts can also influence propagation in the LoVHF band, but these ducts are generally important only for air-to-air or air-to-land transmission (Hitney, et. al, 1985). For this reason they will not be of interest to us.

Ducting will apparently be an important feature of LoVHF propagation only in a few geographical locations. These locations are generally restricted to tropical and semitropical regions located near the interface of land and a large body of water (Patterson, 1982). There is also apparently a higher incidence of these ducts in the spring and summer months (Patterson, 1982).

3. RANGES BEYOND 500 km

For ranges beyond approximately 500 km, there are two modes of propagation: (i) reflections from the F or sporadic E layers and (ii) scattering. The reflected signals tend to be strong, with possible slow interference fading, and the scattered signals much weaker but with rapid fading. The ranges over which these mechanisms operate are largely dependent upon the height above the surface of the earth at which the reflection or scattering takes place. A concise summary of the characteristics of these propagation modes is given by Jacobs (1969). We will first consider reflection mechanisms.

Absorption of waves in the LoVHF band due to passage through the troposphere is negligible (Matthews, 1965). However, absorption losses can be considerable in the ionosphere. Since all modes of propagation for ranges greater than 500 km must pass through the ionosphere, it is appropriate that we discuss this effect here.

Normal absorption can be divided into deviative and nondeviative absorption. Nondeviative absorption occurs predominantly in the D region, where the collision frequency takes on its largest value in the ionosphere and the index of refraction is near one. Deviative absorption occurs primarily near the level of reflection. It is largest in those regions where the progress of the wave is particularly slow. For this reason, when the wave is

reflected from regions near the peak of the E and F layers, the deviative absorption will be large. The degree of absorption is proportional to the collision frequency and the electron concentration, and these factors are functions of the solar zenith angle, the season, geographical location, and sunspot number. Absorption generally increases with sunspot number and decreases with solar zenith angle (Davies, 1965). The seasonal differences are primarily accounted for by differences in the solar zenith angle; however, in the midlatitudes the winter absorption tends to be higher than expected (Davies, 1965). This winter anomaly is apparently explained by the fact that during the summer, layer heights are higher than they are in the winter, thereby causing the path length of rays through the D region to be longer in the winter than in the summer (Laitinen and Haydon, 1962). Because of the difference in the ray path and index of refraction, the absorption is also a function of the polarization of the wave.

In addition to the normal absorption in the ionosphere, there also exists a component that is less predictable. This component is generally a function of solar activity. There are three principal effects which can be identified (i) sudden ionospheric disturbances (SIDs), (ii) ionospheric storms, and (iii) polar cap absorption events (PCAs). SIDs can increase the level of absorption in the D level to the extent that no HF signal is reflected from the ionosphere. These events are referred to as HF blackouts. The onset of these events is often, but not always, rapid. The period of blackout extends from minutes to several hours, and the rate of occurrence is highly correlated with sunspot number (Davies, 1965). Ionospheric storms are generally associated with magnetic storms. During magnetic storms the magnitude of the earth's magnetic field can vary by as much as a few percent. The intensity of

these storms increases with sunspot number and proximity to the auroral region. The most prominent feature of ionospheric storms is the depression of the value of the maximum plasma frequency foF2 and the increased absorption in the D region (Davies, 1965). In the auroral regions the depression in the value of foF2 can range from 30% to 50%; however, for geomagnetic latitudes less than about 45 deg the depression is less than about 10%. The duration of these depressions can range from about 20 to 40 hours (Davies, 1965). This variation in the value of foF2 can have a considerable effect upon propagation, particularly for frequencies near the maximum usable frequency (MUF). Blackouts caused by these storms are most probable in the mornings and least probable in the evenings (Davies, 1965). They occur with about equal probability in the winter and summer and are most likely to occur during the equinoxes and in regions associated with the visual aurora (Davies, 1965). The majority of polar blackouts last less than 6 hours; however, polar blackouts caused by PCA events can last from 1 to 10 days (Davies, 1965). These events are not particularly correlated with either auroral or magnetic activity, but instead are more likely to occur in the geographic polar regions and at times of high sunspot number (Davies, 1965).

3.1 SPORADIC E

The existence of sporadic E propagation, because of its variable nature, is studied mostly by statistical means. The layers responsible for sporadic E propagation are primarily confined to the E layer between heights of 90 and 120 km and appear in horizontal layers of increased ionization density (Davies, 1965). On some occasions the layers are very thin or patchy and mainly serve to scatter the wave as it passes through the layer. At other times the layers are sufficiently thick and widespread to shield the upper

layers of the ionosphere from below (Davies, 1965). They are generally about 1 km thick with a horizontal spread of about 100 km (CCIR Report 259-4, 1978). One European study found that three-fourths of the sporadic E events last less than 2 min, while the total duration of sporadic E was largely due to events which lasted longer than 3 min (CCIR Report 259-4, 1978). In all cases the thickness of the sporadic E layers is less than about 5 km (Al'pert, 1973).

There are three major sporadic E zones: equatorial, temperate, and auroral (CCIR Report 259-4, 1978). The equatorial zone extends in a belt about 6 deg geomagnetic latitude on either side of the geomagnetic equator. In this region sporadic E is generally a daytime phenomenon. These layers are highly transparent, and propagation due to them is primarily accomplished by scattering. The temperate zone extends from the equatorial zone up to about 60 deg geomagnetic latitude. Intense sporadic E reflections are obtained in this region, particularly during the summer. Maximum occurrence is obtained at about 10:00 local time, with a second peak occurring in the afternoon or evening (CCIR Report 259-4, 1978). There is considerable geographic variation in the occurrence of sporadic E, with regions in the Far East exhibiting the greatest occurrence (Smith, 1976). Its frequency of occurrence is apparently associated with thunderstorm activity that penetrates the tropopause (Stewart, 1984, CCIR Report 259-4, 1978) and is relatively insensitive to sunspot number (Jacobs, 1969, CCIR Report 259-4, 1978). In the auroral zone the dominant feature is the nighttime peak in occurrence of sporadic E (CCIR Report 259-4, 1978). Its occurrence is associated with aurora and the magnitude of the sunspot number (CCIR Report 259-4, 1978, Jacobs, 1969).

Let us first examine the ability of sporadic E layers to reflect waves in the LoVHF band. Assuming that the reflecting layers are well modeled by a parabolic layer, we can use the theory of Appleton and Beynon (1947). Using

the graphs constructed by them, we observe that, in order for the ray to be reflected, the value of the ratio of the frequency f to the maximum plasma frequency of the sporadic E layer, foES, must be less than about 6. This means that for values of foES less than about 5 MHz, the incident field will not be reflected from the sporadic E layer. Worldwide, there is approximately a 98% probability that foES will not exceed 10 MHz (Smith 1976); hence, the usable frequency range for sporadic E propagation in the LoVHF band is between 30 and 60 MHz. This is not meant to imply that frequencies outside this range will not be affected by the sporadic E layers, but rather that the signals will be only partially reflected or scattered, with the signal strength greatly reduced (Miya et al., 1978). An examination of figure 12 of Miya et al. (1978) shows that, for a value of foES equal to 10 MHz and a frequency of 80 MHz, the maximum value of the received signal would be about 50 dB below the free space value. This result along with the fact that ham operators have successfully communicated using sporadic E at frequencies exceeding 100 MHz (Stewart, 1984) indicates that limiting sporadic E propagation to frequencies less than 60 MHz is almost certainly too strict a constraint. However, the mechanism of propagation at these higher frequencies, whether by partial reflection or scattering, is unclear, and the description of the received signal will critically depend on the particular mechanism involved. Suffice it to say that the variety of propagation modes that are lumped together under the heading of sporadic E are manifold (Davies, 1965). Sporadic E is believed to affect wave propagation for frequencies up to 90 MHz in the polar and equatorial regions and for frequencies from about 83 to 135 MHz in the temperate zone (CCIR Report 259-4, 1978).

For frequencies greater than foES, there is a distance from the transmitter over which no sky wave is propagated. This region is referred to

as the skip zone. The skip zone will be smallest for the largest value of foES and the smallest value of f. If we take the maximum value of foES to be 10 MHz, this corresponds to a minimum value of the ratio of f to foES equal to 3. From figure 12 of Appleton and Beynon (1940), we observe that for a ratio of f to foES equal to 3, the angle that the ray makes with the vertical at the surface of the earth is about 75 deg. Using figure 2 of Miya et al. (1978), we find that this corresponds to a skip distance of about 500 km. The maximum elevation angle will be somewhat larger than the elevation angle of the ray associated with the skip distance, but for a typically thin sporadic E layer this difference is small. Consequently, for ranges less than about 500 km and for rays with elevation angles significantly greater than about 15 deg, sporadic E layers will not yield high signal strengths. From figure 2 of Miya et al. (1978), we observe that the maximum single-hop range, corresponding to reflection from a height of 130 km, is less than 2700 km. This result is in close agreement with the experimentally observed maximum single-hop distance of 2600 km (Miya et al., 1978). Multihop sporadic E is possible, but its occurrence is much less frequent (CCIR Report 259-4, 78).

In those instances where sporadic E propagation is associated with partial reflection or scattering, the received signal will be weaker than in the case where total reflection is involved. The received signal will be on the order of 20 to 60 dB below the value of the totally reflected signal (Miya et al., 1978, Frank, 1969). In addition, if scattering is involved, the signal will exhibit an increased fading rate, with fading rates increasing from 0.01 to 0.1 Hz, for specular reflection, to 0.05 to 0.4 Hz, for scattering (CCIR Report 259-4, 1978). Radio amateurs operating in the U.S. at frequencies in the LoVHF band have successfully communicated over distances

exceeding 1000 km, using backscattering from irregularities of electron ionization density that are aligned along the earth's magnetic field (Kneisel, 1982). The existence of these irregularities is associated with the occurrence of sporadic E and is a nighttime phenomenon (Kneis, 1982).

3.2 PROPAGATION VIA F LAYER REFLECTION

When propagation via the F layer occurs, the received signal strength will be on the order of the free space value. In order for this to occur, the value of the maximum plasma frequency of the F2 layer, foF2, must be sufficiently large to reflect rays propagating in the LoVHF band. In this regard, the value of the MUF for a given range is of interest. As the frequency increases, the size of the skip zone increases. When the frequency is equal to the MUF, the receiver is located at the edge of the skip zone. Any further increase in frequency will place the receiver inside the skip zone of the transmitter. The value of the MUF is to be distinguished from the maximum observable frequency (MOF). Because of the existence of other propagation modes, the value of the MOF is generally larger than the value of the MUF (Davies, 1965). For example, it is possible for a signal whose carrier frequency is greater than the MUF to be received within the skip zone by a sporadic E reflection.

In order to evaluate the importance of F region propagation for the LoVHF band, we require knowledge of the maximum value of the MUF, and this corresponds to the minimum value of foF2 that will support reflection from the F layer for the LoVHF band. The higher the peak of the F2 layer HmF2, the higher the minimum value of foF2 required to reflect a wave in the LoVHF band (Appleton and Beynon, 1947). The values of HmF2 and foF2 vary over a wide range as functions of geographical location, season, time of day, and sun spot

number. HmF2 and foF2 generally decrease as the distance from the geomagnetic equator increases, and they tend to decrease as temporal distances from local noon increase (Al'pert, 1973). Both HmF2 and foF2 tend to increase for increasing solar activity (Al'pert, 1973). The daytime values of foF2 are generally smaller in summer than in winter and the nighttime values larger in the summer than in winter (Al'pert, 1973, Jacobs, 1979). These effects are especially prevalent in the midlatitudes (Al'pert, 1973). HmF2 typically takes on its minimum values in the winter months (Al'pert, 1973). Using the value of HmF2 and figure 8 of Appleton and Beynon (1947), we can approximate the maximum value of the MUF. Appleton and Beynon's results can be approximately obtained by assuming that the minimum value of the index of refraction times the radial distance r occurs at the peak of the layer. Doing this we obtain

$$\mathrm{MUF} = \mathrm{foF2}\ \frac{1}{\left[1 - \left(\frac{a}{\mathrm{HmF2}+a}\right)^2\right]^{1/2}}\ , \tag{3}$$

where a is the radius of the earth. Using this approach and the average data given by Al'pert (1973), we can obtain some typical values of the MUF. During a solar minimum of activity the MUF is generally below 30 MHz except near noon at the geomagnetic equator, where its average value is about 32 MHz. Nevertheless, measurements show that even in low sun spot years, the MUF can achieve values near 40 MHz in the early evening hours during the spring and fall (Roberts and Rosich, 1971a). During a solar maximum of activity the maximum value of the MUF is greater than 30 MHz over the entire earth, except in the polar regions, all of the time. At these times the MUF can achieve values of 50 MHz in the temperate zone and 60 MHz in the equatorial region (CCIR Report 259-4, 1978). The highest values of the maximum MUF will occur

during the daytime in temperate zones and in the afternoon and early evening hours in the equatorial zone (Jacobs, 1969). During the period of greatest solar activity in recorded history, from 1957-1959, reception at 50 MHz by radio hams was frequent and strong (Jacobs, 1979). However, generally the maximum value of the MUF is confined below 45 MHz for a 4000-km path (Matthews, 1965). The maximum value of the sun spot number averaged over all recorded solar cycles is approximately 110 (Jacobs, 1979). Under these conditions, the MUF is generally confined between 30 and 40 MHz during the daytime hours everywhere except in the polar regions (Roberts and Rosich, 1971b).

The range over which F layer propagation is important depends on the frequency of propagation and the values of foF2 and HmF2. The values of HmF2 vary from about 300 km, during low sun spot years in the midlatitudes, to about 450 km, during high sun spot years in the equatorial regions (Al'pert, 1973). Using equation (3) or figure 8 of Appleton and Beynon (1947), we find that the maximum value of the MUF divided by foF2 varies between about 2.8 and 3.4. Using figure 1 of Appleton and Beynon (1947), we conclude that these results correspond to maximum single-hop ranges between 4000 and 6000 km. It is worth noting that these values are associated with a ray whose elevation angle is zero. However, there are rays associated with larger ranges. These rays are called Pedersen rays. They are reflected from regions near the maximum of the layer and, consequently, have very long delay times and are usually too weak to observe. However, they have been observed quite strongly at distances up to 5300 km (Kift, 1960). It is believed that the range of the Pedersen ray is unstable at these long distances; hence, they may be an important factor in deep fading.

The smaller the ratio of the frequency to foF2, the smaller will be the skip distance. The maximum value of foF2 ranges from about 15 MHz in the equatorial region, to about 10 MHz in the midlatitudes (Al'pert, 1973). From figure 2 of Appleton and Beynon (1947), we find that these results correspond to skip distances at 30 MHz of between 1500 to 2000 km. These results are in agreement with the minimum distance of 1800 km given by Jacobs (1979).

We conclude that during high sun spot years for ranges between 1800 to 6000 km and frequencies less than about 45 MHz, F layer propagation will often be the dominant propagation mode. However, in the equatorial region, and particularly during the spring and fall in the evening hours, F layer propagation may always exist for frequencies below 40 MHz.

The depth of fading for frequencies below the MUF can be quite severe (Davies, 1965). It can be caused by multipath variations between different rays, polarization fading, temporal fluctuations in the absorption, focusing, and temporary disappearance of the signal due to a change in the MUF (Davies, 1965). The deep fading is a consequence of the interference of many rays of comparable strength. These rays include single-hop ordinary (O) and extraordinary (X) rays and multihop O and X rays. Because of the existence of multihop rays, bandwidths are more severely constrained for frequencies less than the MUF than for higher frequencies, especially for long transmission paths. For single-hop transmission, fading rates are about 0.1 Hz, with the rate increasing with frequency, and the spread in delay times is less than a few hundred microseconds (Schwartz et al., 1966). However, for multihop transmission, time delays are on the order of several milliseconds, thus reducing bandwidths to less than 500 Hz (Stein and Jones, 1967).

3.3 SCATTERING MODES

The scattering modes which we will discuss are (i) D and E region scattering, (ii) auroral region scattering, (iii) meteor burst scattering, (iv) transequatorial propagation, and (v) F region scattering. The first three mechanisms are associated with scattering from heights of about 75 to 135 km; hence, the ranges over which they are effective are similar. The last two are associated with scattering in the F region. Because the scattering height is considerably higher for these mechanisms than for the first three, their effective ranges are considerably longer and tend not to overlap with the ranges of the first three. These scattering processes become particularly important just above the MUF, where they may be the only propagation modes available. Hence, they represent a means of extending the MUF to higher frequencies.

There are several scattering mechanisms involved here. Generally weak scattering is associated with scattering in D, E, and F layers. Scattering from both the aurora and meteor trails can often be described by a weak scattering process. Weak scattering for frequencies sufficiently above the MUF is adequately described by Booker and Gordan (1950). The results of weak scattering theory indicate that the scattered signal will decrease with increasing scattering angle and frequency. The reduction of field strength with scattering angle effectively limits the minimum range over which communication is possible. The spread in arrival times and, hence, the bandwidth is limited either by the beamwidths of the transmitting and receiving antennas or by the effective scattering angle and the curvature of the earth (Booker and DeBettencourt, 1955).

Strong scattering from the E layer is generally associated with sporadic E and will not be discussed in this section. Scattering from meteor trails and the aurora are, at times, best described by a reflection process. F region scatter during periods of F spread may involve multiple scattering, strong scattering, or both. Transequatorial propagation is a complex process which may include multiple scattering, coherent scattering, refraction, and ducting.

3.3.1. D and E Region Scattering

The strength of the scattered signal decreases rapidly as the scattering angle increases (Matthews, 1965). Hence, the minimum range is constrained by the large scattering angle involved, and the maximum range is constrained by the height of the scatterers. As the frequency increases, the scattered signal decreases due to scattering from weaker irregularities at a rate on the order of f^{-6} (Davies, 1965). However, this frequency dependence is apparently a function of time of day and has been reported to range from f^{-4} to f^{-12} by Bailey et al. (1955). They found that the signal strength generally varies as f^{-8} near midday and as f^{-7} at other times. The height of D layer scattering is confined to heights of about 70 km during the daytime and between 85 and 90 km at night (Davies, 1965, Matthews, 1965, Bailey et al., 1955). These restrictions generally confine the usefulness of D layer scattering to ranges between 1000 to 2000 km and to frequencies between 30 to 60 MHz (Davies, 1965, Bailey et al., 1955).

Due to the average and random motion of the scatterers, the spectrum of the received signal is both Doppler shifted and spread. As a consequence, the received signal fades at a rate of from 0.2 to 5 Hz, with the fading rate increasing with frequency (Davies, 1965, Bailey et al., 1955). In addition,

the spatial extent of the effective scattering region produces multipath effects.

The maximum occurrence of D layer scattering appears to take place during the summer near noon, and the signal strengths tend to be larger in the arctic and equatorial regions (Davies, 1965) than in the midlatitudes (Bailey et al., 1955). The weakest signals are recorded during the equinoxes in the midlatitudes and from February to April in the arctic region (Bailey et al., 1955). For frequencies in the LoVHF band the increased absorption during periods of HF blackout is more than compensated for by the increased intensity of the scattered signal (Davies, 1965).

3.3.2 Auroral Scattering

Communication by backscattering from the aurora has been used successfully by radio amateurs since the 1940's (Lange-Hesse, 1968). The scattered signals exhibit a strong aspect sensitivity (Lange-Hesse, 1968). One explanation for this is that Bragg scattering, from aurora aligned along the earth's magnetic field, favors those scattering angles such that the difference between the incoming and outgoing wave vector is perpendicular to the earth's magnetic field (Egeland, 1962). Because the auroras are of finite length, the scattered signal will be spread over a few degrees about the Bragg scattering angle. This explanation has been somewhat verified by observations, except for occasions where the auroral ionization is overdense and weak scattering is not a valid approximation (Lange-Hesse, 1968). During periods of particularly strong auroras the signals may appear to come from a variety of directions spread about the north (Lange-Hesse, 1968). The height at which auroras occur is between 75 and 135 km (Davies, 1965). As the height of the aurora increases, the farther to the north must the scattering center

be in order to satisfy the Bragg condition for a particular transmitter and receiver. Hence, because the occurrence of auroras increases with increasing geomagnetic latitude, the probability of reception increases with increasing height of the aurora (Lange-Hesse, 1968). However, as the height of the aurora increases, the maximum range of transmission decreases (Lange-Hesse, 1968). Because of the restrictions placed on the scattering mechanism by the Bragg condition, the region over which reception will take place is difficult to calculate. With low-power transmitters, the Bragg condition must be closely satisfied; but with high-power transmitters this is less of a restriction (Lange-Hesse, 1968). Reception over a particular communication link is subject to sudden change due to variation in the height of the aurora and the magnetic activity. During geomagnetic storms the dip angle of the earth's magnetic field can vary by as much as 1 deg, causing considerable variation in the range of communication (Lange-Hesse, 1968). Nevertheless, radio amateurs have successfully communicated by auroral backscatter with low-power transmitters over distances exceeding 1000 km (Lange-Hesse, 1968). The frequency of occurrence of such transmissions increases with increases in geomagnetic latitude. At geomagnetic latitudes above 70 deg, communication by auroral backscattering takes place, on the average, every second or third day; however, at geomagnetic latitudes near 50 deg it may only occur two to five times a year, with the probability of occurrence greatly increasing with increasing geomagnetic activity (Lange-Hesse, 1968). Occurrences of auroral backscattering communication follow visual observation of the aurora and occur most frequently during the equinoctal periods, particularly in the autumn (Lange-Hesse, 1968).

The received signal is characterized by rapid fading and amplitudes that exhibit a strong frequency dependence. The fading rate can be as high as several hundred hertz, with the rate decreasing with frequency (Lange-Hesse, 1968). The power of the backscattered signal varies as f^{-7}; consequently, propagation in the LoVHF band for frequencies just above the MUF is greatly favored (Lange-Hesse, 1968). In this way interference with powerful refractive modes is avoided, while the scattered signal strength is simultaneously maximized. The signal strength increases with geomagnetic activity. Sudden ionospheric disturbances (SIDs) and polar blackouts are associated with increased electron concentration and absorption in the D region (Bailey et al., 1955). The net effect of these changes in the ionosphere is to reduce the scattered signal for frequencies below the VHF band and to enhance the scattered signal for frequencies above the HF band. During polar blackouts the HF signal fades out completely for periods up to 6 hours or more (Bailey et al., 1955). Polar blackouts last longer and have a more severe effect upon HF propagation than SIDs, while signal enhancement for frequencies above the HF band is greater for polar blackouts than for SIDs (Bailey et al., 1955). It can be stated that, in general, in the VHF band signal strengths are larger than normal when absorption is greater than normal (Bailey et al., 1955). This is a point well worth considering when designing communication systems for operation in the auroral region.

3.3.3 Meteor Burst Communication

The investigation of meteor burst communication was actively pursued in the 1950's; however, with the advent of satellite communication it has been largely ignored (IEEE Spectrum, 1985). Today, its possibilities are again

being actively pursued by both the U.S. Government and private industry (IEEE Spectrum, 1985).

Meteors of many different sizes enter the atmosphere and generally produce ionized trails of lengths approximately equal to 15 km at heights of from 80 to 120 km (Davies, 1965). It is possible, either by reflection from overdense trails or by scattering from underdense trails, to communicate through the use of these meteor trails. With time the electrons in the ionized trail diffuse; hence, the usefulness of a particular trail decreases with time. Generally, the larger the meteor, the longer the duration of communication, the greater the ionization density, and the longer the interval between bursts (Jones, 1981). Using broadbeam antennas, transmission via overdense trails occurs on the average of once a minute. Such trails are able to support communication for about one-half minute. However, underdense trails occur much more frequently; therefore, they are of great importance for meteor burst communication despite the fact that signals scattered from them are weaker (Jones, 1981). The signal reflected from overdense trails is on the order of a thousand times greater than the signal scattered from underdense trails, but the reflected signal suffers from interference effects due to reflection from different parts of the trail (Jones, 1981).

There is a substantial diurnal variation in the characteristics of meteor burst communication. The motion of meteors is concentrated in the plane of the earth's orbit, and they travel in the same direction about the sun as does the earth (Davies, 1965). Because of the motion of the earth about the sun, there exists a minimum rate of the arrival of meteors at 6 p.m. and a maximum at 6 a.m. (Davies, 1965). The average velocity of the meteor follows a similar pattern for the same reason (Davies, 1965). This is important because

meteors with larger velocities produce trails at greater heights and, because of the slower diffusion time at such heights, consequently produce trails of longer duration (Davies, 1965). Hence, the distribution of trail heights and duration times also follows a diurnal variation. Finally, because of the motion of the earth about the sun, most meteors will appear to arrive from the direction of the morning hemisphere (Davies, 1965). Due to the constraints imposed on the optimal communications link by the reflection process or Bragg scattering, the geometry of reception is highly constrained. As a consequence, for a particular communication link, there will exist in the sky a particular "hot spot," where scattering or reflection is favored (Davies, 1965). Due to the diurnal variation of the characteristics of the meteor bursts, the location of this "hot spot" will also have a diurnal variation.

Aside from the occurrence of meteor showers and the diurnal variation of meteor arrival, there also exists a monthly variation in meteor arrival. Apparently, meteors are distributed about the orbit of the earth in such a way as to produce a maximum of arrivals in July and August and a minimum in February (Jones, 1981). Meteor showers are also prevalent in the period from June through August, with some also occurring over the period transmission frequencies require higher meteor trail electron concentrations for comparable signal strength; hence, because meteor trails producing these conditions are less likely to occur, the probability of successful transmission decreases (Davies, 1965). Furthermore, because for a given signal strength the required electron concentration increases as the frequency increases, the duration of reception, for a given meteor trail will decrease with frequency. These limitations require that the frequency of propagation be less than about 110 MHz (Davies, 1965). For frequencies just above the MUF, interference with F

region reflection will be avoided; hence, for frequencies between the MUF and about 110 MHz, meteor burst communication is possible.

Because of the aspect sensitivity of the scattered or reflected signal, range limitations are difficult to assess. The height at which the meteor trails occur limits the range to less than about 2300 km; however, adequate communications links are likely to exist at ranges much less than this. One communications link was maintained in the early 1960's over a distance of 1300 km at a frequency of 50 MHz with a loss of about 80 dB above that of free space. This system was capable of a teletypewriter transmission rate of 40 words per minute at a character error rate of 0.35 percent (Davies, 1965). A portable meteor burst communication system using backscattering from overdense meteor trails has successfully communicated in the LoVHF band over distances ranging from line of sight to 200 miles (Jones,1981). Jacobs (1979) lists the range of communications links for radio amateurs at between 800 and 1200 miles. Under more or less ideal geometric conditions, the signal scattered from meteor trails is commonly many decibels greater than that from D and E region scattering. In addition, the intensity of the scattered field appears to decrease more slowly with frequency than the D and E region scattered fields (Bailey et al., 1955).

Reflection from the heads of meteors or, more commonly, from rapidly lengthening meteor ionization trails can produce large Doppler shifts. However, the Doppler shifts produced by the drift velocities of the meteor trails are typically on the order of a few hertz (Bailey et al., 1955). Overdense and long-lasting trails tend to break up into multiple scattering centers, producing fading rates on the order of 1 to 10 Hz and pulse spreading on the order of 10 μs (Sugar, 1964). Underdense trails with shorter durations exhibit almost no Doppler or time spreading (Sugar, 1964).

3.3.4 Transequatorial Propagation

Transequatorial propagation (TEP) occurs, as the name implies, across the geomagnetic equator. Its range is generally confined to propagation between regions roughly 1500 to 2500 miles above and below the geomagnetic equator (Tilton, 1968). There are at least three modes of propagation associated with TEP. The first type is associated with the anomaly in electron concentration that occurs at geomagnetic latitudes of ±20 deg during the afternoon and early evening (Heron, 1981, Davies, 1965). This anomaly exhibits higher density of electron concentration both north and south of the geomagnetic equator. As a consequence, a ray can be directed by these tilts, without an intervening ground reflection, to ranges exceeding 5000 km (Ferguson and Booker, 1983). The signals propagated by this mode are generally confined to frequencies less than about 60 MHz and exhibit high field strengths and slow fading (Heron, 1981). This type of TEP is favored by an F layer which is symmetrical about the geomagnetic equator. For this reason, propagation at the equinoxes is preferred (Heron, 1981). At these times, the larger the value of foF2, the larger will be the frequency which can propagate via this mode. For this reason, propagation by this mode is favored in the afternoon during years of high solar activity (Heron, 1981, Nielson, 1969).

The second type of TEP is associated with scattering from bottomside disturbances in the electron concentration and with propagation at frequencies above 50 MHz (Ferguson and Booker, 1983). It is highly correlated with range-type spread F and not with frequency-type spread F (Heron, 1981, Rastogi and Woodman, 1978, Cohen and Bowles, 1961). As a consequence, its occurrence is most frequent at night during times of high sun spot number at the equinoxes (Heron, 1981). This type of TEP is characterized by rapid fading

from 10 to 20 Hz (Nielson, 1969, Davies, 1965) and Doppler shifts consistent with an east-to-west motion of the scatterers of about 100 m/s (Davies, 1965). The signal amplitude has values on the order of 50 dB below that of free space at 90 MHz over paths on the order of 4000 km, with signal strengths rapidly increasing with decreasing frequency (Nielson, 1969). The signal strengths are stronger than one would expect by scattering from weak irregularities of electron density (Ferguson and Booker, 1983, Nielson, 1966). Since the irregularities are aligned along the earth's magnetic field, it has been suggested that a type of focusing of the scattered signal could take place (Ferguson and Booker, 1983). The range of propagation is generally confined to distances less than 5000 km and to frequencies between 50 and (100 MHz (Ferguson and Booker, 1983).

The last type of TEP is associated with the existence of underdense plumes or ducts that are aligned along the earth's magnetic field. It is suggested that the gradients of the index of refraction along these plumes is great enough to act as a waveguide (Heron, 1981, Cracknell, 1980). As the frequency increases, the gradient of the index of refraction will decrease; hence, there will be a marked decrease in the ability of these ducts to support propagation at higher frequencies (Heron, 1981). This result is consistent with the observed falloff in signal strength with frequency for TEP. It has been suggested that this mode of propagation is most likely responsible for TEP in the VHF band (Heron, 1981, Cracknell, 1980). Cracknell (1980) suggests that, in addition, spread F plays an important role in the operation of this mode. The irregularities that exist under spread F conditions serve to increase the angular spread of the incident field. Though the effect of this scattering is to weaken the field, it also increases the

probability that the incident field will lie within the acceptance cone of the duct (Cracknell, 1980). The existence of these irregularities can also explain the complicated fading pattern associated with TEP (Cracknell, 1980). Spread F could also have a similar affect on the first type of TEP (Cracknell, 1980).

3.3.5 F Region Scatter

Attempts to observe F region scattering from irregularities of ionization density outside the equatorial region have been unsuccessful (Bailey, 1962). Propagation from Cedar Rapids, Iowa, to Bermuda via F region scatter was unsuccessful even in the presence of spread F at the path midpoint (Bailey, 1962). Within the equatorial region (about $\pm$20 deg geomagnetic latitude) the scattered signals show a marked aspect sensitivity, which points to the alignment of the irregularities along the direction of the earth's magnetic field (Bailey, 1962). However, paths which would appear to have a similar geometric advantage can have large differences in signal strength (Nielson, 1966). The scattering theory proposed by Ferguson and Booker (1983) has apparently resolved this discrepancy, attributing it to coherent scattering from the field-aligned irregularities (Ferguson, 1984). This theory can also explain the observation that the scattered signal arrives from a direction outside the great circle path (Bateman et al., 1959) as resulting from the fact that the stationary points are frequently located outside the meridian of the transmitter and receiver (Ferguson, 1984).

The reduction in strengths of the received signals relative to the normal E layer scatter is about 30 to 40 dB at 50 MHz and 40 to 50 dB at 36 MHz (Bateman et al., 1959). The fading rates of about 5 Hz at 50 MHz are similar

to that of normal E layer scattering (Bateman et al., 1959). The spread in arrival times is on the order of several hundred microseconds (Bateman et al., 1959). The occurrence of F region scattering is generally correlated with the occurrence of spread F. It could be said that F region scatter and bottomside-scattering TEP are different manifestations of the same phenomenon, the only difference being that the transmitter and receiver are not located across the geomagnetic equator. According to the theory of Ferguson and Booker (1983), this should result in much weaker signals.

4. MODELS

Our objective is to be able to describe the field strength and path loss for transmission in the LoVHF band. Due to the highly variable nature of the propagation modes, the models used must be at least partially statistical in nature. These models can be used by operators of communication transmitters and radars to aid them in determining the likelihood of radar detection and signal reception and interception. Quite a few models of varying degrees of complexity and flexibility already exist. By carefully selecting from among these existing models, it should be possible to satisfy the needs of most users.

Before describing these models, it is important that the meaning of various terms be clear. System loss is defined as the ratio of the input strength to the output strength. Depending upon at what point in the communications link the input and output strengths are measured, system loss can have many different meanings. Generally, the input and output strengths (P_T and P_R, respectively) are measured in terms of average power, and the system loss expressed in decibels [. More explicitly, we have that

$$10 \log(P_R) = 10 \log(P_R) - \Gamma, \tag{4}$$

where log stands for the logarithm to the base ten. Since the power output is less than the power input, Γ is a positive quantity. If the input or output power is measured at some point within the transmitter or receiver, then transmitter or receiver losses must be taken into account.

Path loss is determined by comparing the radiated power of the transmitter with the power delivered across the input impedance of the receiver. Hence, path loss is affected by the characteristics of the receiving antenna. In this case, the power received, P_R, can be written as

$$P_R = \frac{E^2}{Z_0} A_R(\Omega) \ , \tag{5}$$

where E is the average electric field incident from a solid angle Ω, A_R is the effective aperture of the receiving antenna, and Z_0 is the impedance of free space (about 120 π). In general, A_R includes the effects of polarization and impedance mismatch. If the incident field is not described by a unique direction of arrival, a sum over all angles of arrival must be performed. For a polarization- and impedance-matched receiver

$$A_R(\Omega) = \frac{\lambda^2}{4\pi} G_R(\Omega) \ , \tag{6}$$

where G_R is the gain of the receiver relative to an isotropic antenna. Generally this relationship is used, and the losses due to polarization and impedance mismatch are explicitly taken into account separately. Sometimes the input voltage to the receiver V is related to the incident electric field E by the use of an effective antenna length L and the relationship EL = V. In either case, it is possible, if the characteristics of the receiving antenna

are known, to determine the field strength E from the power delivered to the input impedance of the receiver.

Often it is desirable to describe losses in terms that are independent of the characteristics of the transmitting and receiving antennas. For example, radar operators would be more interested in the field strength at a given range than in the power received by an antenna located at that range. In this case, all losses are due to the effects of the propagation medium or channel. We will call this loss the basic transmission loss.

It is convenient to isolate from the basic transmission loss the effect of free space propagation. In free space the average electric field E propagated into a solid angle Ω is given by

$$E^2 = \frac{P_T G_T(\Omega) Z_0}{4\pi R^2} \quad . \tag{7}$$

Here, P_T is the average transmitted power, $G_T(\Omega)$ is the gain of the transmitter relative to an isotropic antenna, and R is the distance from the transmitter. Hence, the free space field expressed in decibels above 1 μV/m is given by

$$20 \log E = 104.8 + 10 \log(P_T) + 10 \log(G_T) - 20 \log (R), \tag{8}$$

where P_T is expressed in kilowatts and R in kilometers, and the free space loss Γ_{fs} is given by

$$\Gamma_{fs} = 71.0 + 20 \log(R) - 10 \log(G_T) \quad . \tag{9}$$

With the essential terms now defined, we can proceed with the description of available models. We found it convenient, when describing the various factors which affect the propagation of waves in the LoVHF band, to distinguish between those factors which are influential at ranges less than and greater than 500 km. We will find it convenient to make a similar distinction here.

4.1 RANGES LESS THAN 500 km

For distances beyond the radio horizon and with systems employing broadbeam antennas, reflections from the aurora and meteor trails can be important modes of propagation. However, for troposcatter systems, the region of intersection of the transmitting and receiving antenna patterns is located below the ionosphere; hence, backscattering from either the aurora or meteor trails is virtually eliminated. For those systems employing ducting as a means of propagation, the majority of the transmitted power is confined to low elevation angles; hence, backscattering from the aurora and meteor trails can be avoided. Meteor burst systems have been designed to operate at ranges less than 500 km (Jones, 1981). Because they use broadbeam antennas to increase the probability of transmission, they are susceptible to interference from tropospheric modes of propagation. Nevertheless, we will assume that in those cases where auroral and meteor burst backscattering is used, the probability of interference is small and that, consequently, those systems that employ the troposphere as the primary medium of propagation can be considered as distinct from those that do not.

The models that we will examine at ranges less than 500 km are IREPS, PROPHET, SRICOM, the Longley-Rice model, and EPM-73. The IREPS model was designed to be used in predicting field strength and coverage area for ships operating communication systems and radars in the HiVHF band (Hitney et al., 1984). It is the only one of these models which explicitly calculates the ducted field. The SRICOM (Hagn et al., 1982), Longley-Rice (Longley and Rice, 1968), and EPM-73 (Lustgarten and Madison, 1977) models all calculate the basic tropospheric transmission losses. IREPS and PROPHET (Sailors et al., 1983) use the EPM-73 model, while SRICOM uses both the EPM-73 and Longley-Rice

models. Except for PROPHET, these models are primarily of value for ranges less than 500 km.

For ranges less than 500 km, the condition of the troposphere and the surface of the earth are of greatest importance in determining the character of the signal received. The condition of the troposphere can be adequately described by radiosonde data (Hitney et al., 1985). It has been found that the assumption of lateral homogeneity of the troposphere is generally adequate; hence, radiosonde data at one location is sufficient to determine the refractive index profile of the troposphere (Hitney et al., 1985). Without recent radiosonde data, it is possible to create an average refractivity profile for a given month and location from the data stored in IREPS (Hitney et al., 1984).

Other factors which are important in the determination of the field strength are the reflection coefficient of the earth, the existence of various obstacles in the path of propagation, and the heights and characteristics of the transmitting and receiving antennas. With this additional information, it is possible to calculate the field strength and path loss at the receiver. Generally, it is assumed that the receiver is adjusted for maximum signal strength. If this is not the case, additional losses due to polarization and impedance mismatch and loss of gain will have to be included. The effects of obstacles, such as buildings and trees, are difficult to calculate. Some discussion of these effects is given by Hagn et al. (1982). The effects of rough surfaces are somewhat accounted for by the Longley-Rice and IREPS models. IREPS accomplishes this primarily by considering reflection losses over a rough sea (Hitney et al., 1984).

Most models divide ranges of less than 500 km into four regions: (i) the interference region, (ii) the intermediate region, (iii) the diffraction region, and (iv) the troposcatter region. In the interference region the effects of the direct, reflected, and surface waves are dominant. In the diffraction region, if there is no ducted field, the surface wave can be generally neglected, and the field that is diffracted around the curved earth is the dominant field. As the range increases, the strength of the diffracted field decreases until, in the troposcatter region, the signal scattered from the troposphere becomes the dominant mode of propagation. If ducting exists as a mode of propagation, it generally is the dominant mode of propagation in both the diffraction and troposcatter regions. In the mode theory of wave propagation the diffracted and ducted fields are different manifestations of the same modal representation (Budden, 1961a) and can, therefore, be treated simultaneously. In the intermediate region the field is difficult to calculate. For ranges beyond the intermediate region and for frequencies in the LoVHF band, one mode is adequate to describe the field (Hitney et al., 1985). However, within the intermediate region many modes are required, with the number increasing as the radio horizon is approached (Hitney et al., 1985). For this reason the fields in the intermediate region are generally approximated by the method of "bold interpolation" (Hitney et al., 1984, Fishback, 1964). In this method the fields from the interference region are smoothly joined to the fields in the diffraction region. We will now examine the methods available for calculating the field strength in the interference, diffraction, and troposcatter regions.

4.1.1 The Interference Region

For distances within the radio horizon, the predominant fields are due to the direct, reflected, and surface waves (Bullington, 1947). Most models calculate field strengths by using a method similar to that given by Norton (1941), Bullington (1947), Reed and Russell (1964), or Fishback (1964). The general idea can be described by examining the situation in free space over a spherical earth of effective radius R_e. Freehafer (1964) shows that if the antenna heights are much less than the range, this model adequately describes the field in the interference region for propagation over a spherical earth and through a weakly refracting troposphere.

Let the free space electric field E propagated in the plane of the great circle path between the receiver and transmitter be given by

$$E = \left[\frac{P_T Z_0}{4\pi}\right]^{1/2} \frac{f(\phi)}{R} e^{-jkR} , \qquad (10)$$

where ϕ is the elevation angle of the ray measured from the transmitting antenna, $f(\phi)$ is the normalized antenna pattern, R is the distance from the antenna, and k is the wave number. The magnitude of the normalized antenna pattern is related to the gain G_T of the transmitter relative to an isotropic antenna by the relationship

$$|f(\phi)| = [G_T(\phi)]^{1/2} . \qquad (11)$$

When the receiver and transmitter are located on the surface of the earth, there are two principal contributions to the field strength. One is from the direct ray, the other from a ray which is reflected from the earth's surface. The field due to the direct ray E_D is given by

$$E_D = \left[\frac{P_T Z_0}{4\pi}\right]^{1/2} \frac{f(\phi_{D1})}{R_D} e^{-jkR_D} , \qquad (12)$$

where the subscript D stands for direct. The field due to the reflected ray E_R is given by

$$E_R = \left[\frac{P_T Z_0}{4\pi}\right]^{1/2} \frac{D(\alpha)R(\alpha)f(\phi_{R1})}{R_R} e^{-jkR_R} , \qquad (13$$

where α is the elevation angle which the reflected ray makes with the earth's surface, R is the reflection coefficient of the earth, D is the divergence factor due to reflection from a curved surface of radius R_e, and R_R is the total distance of propagation from the transmitter to the receiver. The angles ϕ_{D1}, ϕ_{R1}, and α are functions of the distance between and the heights of the transmitter and receiver. Taking the sum of the direct and reflected waves, we obtain for the total field E_T (Freehafer, 1964)

$$E_R = \left[\frac{P_T Z_0}{4\pi}\right]^{1/2} \frac{e^{-jkR_D}}{R_D}\left[f(\phi_{D1}) + D(\alpha)R(\alpha)f(\phi_{R1})e^{-jk\Delta}\right] , \qquad (14)$$

where $\Delta = R_R - R_D$. For small grazing angles $D(\alpha)$ tends to infinity; hence, this expression for E_T is limited to angles α that are greater than $[\lambda/2\pi R_e)]^{1/3}$ (Norton, 1941). If we can neglect the difference in phase between the two normalized antenna patterns, $f(\phi_{D1})$ and $f(\phi_{R1})$, then equation (14) can be written as

$$E_T = E_0\left[1 + D(\alpha)R(\alpha)\left(\frac{G_T(\phi_{R1})}{G_T(\phi_{T1})}\right)^{1/2} e^{-jk\Delta}\right] . \qquad (15)$$

Because the direct and reflected rays are incident upon the receiver at different angles, their respective gains will be different. The ratio of the

direct and reflected received signal strengths is equal to $f_R(\phi_{D2})/(f_R(\phi_{R2})$, where f_R is the normalized antenna pattern of the receiver, and ϕ_{D2} and ϕ_{R2} are the angles at which the direct and reflected rays are incident upon the receiver. As before, we neglect the phase difference in the ratio of these antenna patterns and obtain for the power P_R received by an impedance-matched receiver:

$$P_R = P_0 \left| 1 + D(\alpha)R(\alpha)\left(\frac{G_T(\phi_{R1})G_R(\phi_{R2})}{G_T(\phi_{D1})G_R(\phi_{D2})}\right)^{1/2} e^{-jk\Delta}\right|^2 , \qquad (16)$$

where P_0 is the free space power received,

$$P_0 = \left(\frac{\lambda}{4\pi}\right)^2 \frac{P_T}{R_D^2} G_T(\phi_{D1})G_R(\phi_{D2}) . \qquad (17)$$

If the antenna heights are much less than the range, the factor involving the ratio of the gains is often near one. Longley and Rice (1968) neglect the divergence factor in their expression for P_R, and in the FORTRAN code supplied by them, the ratio of the gains is set to one. IREPS (Hitney et al., 1984) retains the difference in gain between the transmitted direct and reflected rays but neglects this difference in the reception of these rays.

The reflection coefficient for a smooth earth is equal to the Fresnel reflection coefficient for a plane surface (Bullington, 1947). Assuming that the heights of the antennas are much less than the range, then for all frequencies in the LoVHF band, the reflection coefficient for horizontal polarization is approximately equal to -1 (Kerr, 1964). However, for vertical polarization the situation is more complicated, and the full expression for the Fresnel reflection coefficient must be used. This is the procedure followed by IREPS, in which it is assumed, however, that propagation occurs

over water (Hitney et al., 1984). Values for the earth's complex dielectric constant as a function of frequency are provided by SRICOM (Hagn et al., 1982, and Sailors, et al., 1983).

The Fresnel reflection coefficients and the divergence factor are a function of the elevation angle α. In free space the rays are straight lines; hence, α can be determined as a function of the antenna heights and the effective earth radius by geometry (Hitney et al., 1984).

Reflections from rough surfaces scatter radiation and, consequently, involve an additional loss over that of a smooth surface. The basic assumption of the EPM-73 model is that the surface of the earth is reasonably smooth (Lustgarten and Madison, 1977). Losses due to reflection from a rough surface are generally taken into account by incorporating a multiplicative Gaussian loss factor in the reflection coefficient. The greater the angular spread of the scattered radiation, the greater the loss and the smaller the reflection coefficient in the direction of the specularly reflected component. IREPS uses the Phillips ocean-wave model to determine the mean sea height $\bar{h}$ and then multiplies the Fresnel reflection coefficient by the factor

$$\exp\{-2[k\bar{h}\sin(\alpha)]^2\} \qquad (18)$$

(Hitney et al., 1984). The Longley-Rice model uses a more general technique. It defines a roughness parameter which describes the variation in elevation above or below a least-squares fit to the elevation as a function of range. The difference between those heights which is exceeded 10 percent and 90 percent of the time along the ray's path is the terrain's interdecile range. As the range increases, the interdecile range tends to increase because the possible variations in elevation tend to increase. As the range increases,

the interdecile range tends to approach an asymptotic value that is characteristic of a particular terrain type. Longley and Rice (1968) list these asymptotic values for various terrains and use an empirical fit to determine the interdecile range as a function of range. From this expression they can determine the rms deviation of the terrain heights. They then use this result in a manner similar to that used by IREPS to describe the losses due to reflection from a rough surface (Longley and Rice, 1968). A comparison of results using EPM-73 and the Longley-Rice model indicates that EPM-73, with a considerably simpler method, yields comparable results over flat terrain (Lusgarten and Madison, 1977).

In order to use these results, an expression for the effective earth's radius R_e must be obtained. IREPS obtains this value by actually tracing a ray through the troposphere, using the model of the index of refraction supplied by the user or the average profiles available internally. The change in the height of the ray for a given range of propagation is then used to obtain the same change in height and range for an effective linear medium. Equation (1b) can then by used to determine the effective earth radius. The Longley-Rice model uses a less sophisticated method. The user must supply the value of the refractivity N at sea level. The refractivity is defined by

$$N = (n - 1)10^{-6} , \tag{19}$$

where n is the index of refraction. From the value of N the value of the effective earth radius is given by

$$R_e = \frac{\alpha}{1 - 0.04655 \exp(0.005577N_s)} , \tag{20}$$

where $N_s = N \exp(-0.1057h)$, and h is the height of the lower antenna above mean sea level (Longley and Rice, 1968). The mean value of N can be obtained from

world maps given by Hagn et al. (1982). The advantage of the method employed by IREPS is that the same data used to calculate R_e can also be used in calculating the ducted field.

In addition to the field produced by the direct and reflected rays, there is also the contribution of a surface wave (Norton, 1941). The surface wave in the LoVHF band can generally be neglected for horizontal polarization, but must be included for vertical polarization at heights less than about 5 wavelengths (Bullington, 1947). As the reflection angle α tends to zero, the effect of the surface wave becomes increasingly important. The reason for this is that at near-grazing angles, the reflection coefficient is close to -1, and the phase of the direct and reflected ways is nearly identical; hence, the sum of the direct and reflected waves is near zero, leaving only the surface wave E_{su},

$$E_{su} = \frac{2E_0}{d} A_1 F_s \tag{21}$$

(Norton, 1941, Burrows and Gray, 1941). Here, d is the range over the earth's surface, E_0 is the free space field, A_1 is a plane earth attenuation factor, and F_s is the "shadow factor." The "shadow factor" takes into account the effect of the curvature of the earth's surface (Burrows and Gray, 1941). The factor A_1 is a function only of the earth's complex dielectric constant, the wavelength, and the range, whereas the "shadow factor" F_s is a function of the wavelength, the range, and the effective earth radius. For distances less than about $80/(f_{mc}^{1/3})$ km, where f_{mc} is the frequency in MHz, the "shadow factor" is approximately one (Norton, 1941). In this case we have

$$E_{su} \approx E_0 \frac{4\pi h'_T h'_R}{\lambda d} \tag{22}$$

Here, the effective antenna height h_T is given by

$$h_T' = h_T + \frac{j\lambda}{2\pi Z} , \tag{23}$$

$$Z = (\varepsilon - \cos^2(\alpha))^{1/2}/\varepsilon \tag{24}$$

for vertical polarization, by

$$Z = (\varepsilon - \cos^2(\alpha))^{1/2} \tag{25}$$

for horizontal polarization, and ε is the complex dielectric constant of the earth. h_T is the height of the transmitting antenna. The expression for h_R' is obtained by substituting the height of the receiver for that for the transmitter.

The importance of the surface wave increases with decreasing frequency (Bullington, 1947). For frequencies greater than 100 MHz and antenna heights greater than about 10 m, the influence of the surface wave on the field strength can be neglected (Bullington, 1947). For this reason, both IREPS (Hitney et al., 1984) and Fishback (1964) neglect the effect of the surface wave. However, in the LoVHF band the surface wave is more important than in the HiVHF band, and its effect cannot generally be neglected.

EPM-73 is a semiempirical model which calculates basic transmission loss in the interference region. It makes no distinction between the direct, reflected, and surface waves. However, the low (h/λ) version of the EPM-73 model (Lusgarten and Madison, 1977) does incorporate the effects of the surface wave in its calculation of the basic transmission loss. Here, h is the height of either antenna, and λ is the wavelength. The EPM-73 model assumes an effective earth radius of 4/3 the earth's radius. An improved version of EPM-73, SRICOM, has been designed by Hagn et al. (1982). SRICOM

includes the possibility of an arbitrary effective earth's radius, is valid at larger antenna heights, and uses Bullington's (1947) more accurate expressions for the effective antenna heights (Hagn et al., 1982). The low h/λ portion of EPM-73 is used by PROPHET (Sailors et al., 1983). In the LoVHF band both the high and low h/λ versions of EPM-73 will have to be used. In SRICOM both models are used, and the version which gives the greater loss determines the basic transmission loss (Hagn et al., 1982). The Longley-Rice model takes surface wave propagation into account by extrapolating the value of the field in the diffraction region back into the interference region (Longley and Rice, 1968).

4.1.2 Diffraction and Troposcatter Region

All of the models discussed so far also calculate the loss in the diffraction region. The range at which diffraction becomes the dominant effect can be defined by

$$d_1 = d_{los} + \frac{1.5}{\beta\eta} \quad , \tag{26}$$

where

$$\beta = \left(\frac{1}{\lambda R_e^2}\right)^{1/3} \quad , \tag{27}$$

d_{los} is defined by equation (1a), and η is a complicated function of the complex dielectric constant of the earth, the frequency, and the effective earth radius (Reed and Russell, 1964). Over seawater and for frequencies greater than about 100 MHz, IREPS employs a form for d_1 of

$$d_1 = d_{los} + 230.2 \left[\frac{(R_e/a)^2}{f_{mc}}\right]^{1/3} \quad , \tag{28}$$

where d_1, the earth's radius α, and R_e are expressed in km, and f_{mc} is the frequency in MHz. η generally varies over values from about 1.5 to less than 1.61 (Norton, 1941); consequently, $0.015c^{1/3}/\eta$ is similar to 0.5. Here, c is the speed of light in km/s. The Longley-Rice model uses this approximation to define d_1 by

$$d_1 = d_{los} + \frac{1}{2}\left(\frac{R_e^2}{f_{mc}}\right)^{1/3} \quad . \tag{29}$$

EPM-73 uses a more convoluted means of treating diffraction. In its high h/λ version it makes a clear distinction between the interference and diffraction regions (Lustgarten and Madison, 1977); however, in its low h/λ model no distinction is made. The high h/λ model defines d_{los} for an effective earth radius of 4/3 times the earth's radius. SRICOM modifies d_{los} in its version of EPM-73 to use any value of the effective earth radius (Hagn et al., 1982). For sufficiently small antenna heights, the surface wave represents the principal part of the field in both the interference and diffraction regions. Apparently, the major contribution to the field in the low h/λ is due to the surface wave. In this case, there is no need to distinguish between the interference and diffraction regions. Instead, EPM-73 finds it more fruitful in its low h/λ model to distinguish between the distance at which the earth can be considered flat and the distance at which the effects of its curvature are important (Lustgarten and Madison, 1977).

The Longley-Rice model calculates the diffraction losses by means of analytical methods similar to those presented by Norton (1941) and Bullington (1947). In addition, it attempts to take into account the effect of the surface roughness on the basic transmission loss in the diffraction region (Longley and Rice, 1968).

IREPS calculates the diffracted field as a special case of an evaporation duct with zero elevation height. The method they use to calculate the evaporation duct field strength is based upon a numerical fit to results obtained at 9.6 GHz. The field strength at other frequencies is obtained by an appropriate scaling of both the duct height and range. Since IREPS is intended to be used above 100 MHz, it is not clear whether this method is accurate at frequencies below 100 MHz. However, implementation of the XWVG program in IREPS, as proposed by Baumgartner et al. (1983), would more than adequately remove this possible deficiency. This program calculates field strengths by using the mode theory of wave propagation as given by Budden (1961a). It is capable of calculating and summing a large number of modes. However, as the distance from the radio horizon increases, the number of modes required for a given accuracy decreases. In the diffraction region usually only one mode is required to adequately calculate the diffracted field (Hitney et al., 1984, Fishback, 1964). Consequently, the methods employed in XWVG could be considerably simplified when used for the calculation of the diffracted field.

As the range increases, the diffraction losses increase, and eventually a region is reached where the troposcattered signal is the dominant signal received. Most models that estimate the troposcattered signal strength use an empirical fit to experimental data. The greater the refracting abilities of the troposphere, the larger will be the troposcattered signal. This characteristic of the troposphere is reflected in a larger effective earth radius. As in other regions, IREPS (Hitney et al., 1984) and the Longley-Rice model (Longley and Rice, 1968) include the possibility of an arbitrary value of the effective earth's radius, while EPM-73 assumes a value of 4/3 times the earth's radius.

4.1.3 Ducting

The field propagated through the troposphere can be calculated by using the waveguide theory of wave propagation (Budden, 1961a). This method is equally accurate for ranges less than and greater than the radio horizon; however, it is most useful for calculating field strengths well beyond the radio horizon (Hitney et al., 1985). If the range is less than about an earth radius α and the fields are calculated at a height h above the earth's surface much less than α, then propagation over the surface of a curved earth can be reduced to propagation over a flat earth with a modified index of refraction n_M (Freehafer, 1964). This modified index of refraction is given by

$$n_M = \left(1 + \frac{h}{a}\right)n \ , \qquad (30$$

which is similar to

$$n_M \approx n + \frac{h}{a} \qquad (30$$

(Freehafer, 1964). Here, n is the index of refraction. If the index of refraction is approximately linear, an effective earth radius R_e is defined by equation (1b) and we obtain

$$n_M \approx n_0 + \frac{h}{R_e} \ , \qquad (32)$$

where n_0 is the value of n at the earth's surface. If dn/dh is greater than $-1/\alpha$, R_e is positive and n_M increases with height. The diffracted field was calculated in all the models previously discussed on the basis of assuming that R_e was positive and not near zero. If dn/dh is less than $-1/\alpha$, R_e is negative and n_M decreases with height. As a consequence, it is now possible

for the reflection height to be real and for the signal strength to dramatically increase. This is the situation that exists for ducted signals.

In the troposphere the dielectric constant changes very little over a wavelength in the LoVHF; hence, the depolarization term can be neglected. This means that for both horizontal and vertical polarization, the electric and magnetic vectors can be found from the solution to the equation

$$(\Delta^2 + k^2\varepsilon)\Pi = -S \ , \tag{33}$$

where S is either equal to the dipole moment per unit volume P divided by $\varepsilon_0\varepsilon$ for vertical polarization or the magnetic moment per unit volume M for horizontal polarization. Here, ε is the index of refraction squared, $\varepsilon_0\varepsilon$ is the dielectric constant of free space, and k is the angular frequency w divided by the speed of light c. In general, both Π and S are vectors. However, only the component of Π in the direction of S is important; so only scalar quantities need be considered.

By horizontal polarization we mean that the field is always perpendicular to the direction of stratification. In the flat earth approximation, we assume that the troposphere is horizontally stratified; hence, a horizontally polarized field is always contained within the xy plane (if the z vector is in the vertical direction). In a spherical coordinate system, this means that a horizontally polarized wave only has a ϕ component. A vertically polarized wave has a component in the direction of stratification. For a vertically oriented magnetic dipole the electric field $\vec{E}$ is horizontally polarized and is given by

$$\vec{E} = E_\phi = \frac{jk}{c\varepsilon_0}\frac{\partial \Pi}{\partial r} \ , \tag{34}$$

where E_ϕ is the component of $\vec{E}$ in the ϕ direction. For a vertically oriented electric dipole, the electric field is vertically polarized and the magnetic field is horizontally polarized. The magnetic field $\vec{H}$ is given by

$$\vec{H} = H_\phi = -j\omega\varepsilon_0\varepsilon\frac{\partial\pi}{\partial r} \tag{35}$$

(Fishback, 1964).

In order that the boundary conditions be satisfied at the earth's surface, we require that

$$\frac{\partial\Pi_1}{\partial z} = \frac{\partial\Pi_2}{\partial z} \tag{36}$$

$$\Pi_1 = \Pi_2 \tag{36a}$$

for a horizontally polarized electric field, and that

$$\varepsilon_1\Pi_1 = \varepsilon_2\Pi_2 \tag{37}$$

$$\frac{\partial\Pi_1}{\partial z} = \frac{\partial\Pi_2}{\partial z} \tag{38}$$

for a vertically polarized electric field (Fishback, 1964). Here, the subscripts 1 and 2 refer to those quantities evaluated on either side of the earth's surface.

For a magnetic or vertical dipole of unit strength, S is a delta function which, for convenience, we locate at $\rho = 0$ and $z = z'$. In this case, Π is independent of ϕ and can therefore be written as

$$PI(\rho,z) = \frac{k^2}{4\pi}\int_{-\infty}^{\infty} H_0^{(2)}(ks\rho)\Pi(ks,z)sds\ , \tag{39}$$

where $H_0^{(2)}$ is the Hankel function of the second kind (Baumgartner, 1983). $\Pi(ks,z)$ is the solution to

$$\left[\frac{d^2}{dz^2} + k^2(n_m^2 - s^2)\right]\Pi(ks,z) = -\delta(z - z') \tag{40}$$

above the earth's surface, and the solution to

$$\left[\frac{d^2}{dz^2} + k^2(n_g^2 - s^2)\right]\Pi(ks,z) = 0 \tag{41}$$

below the earth's surface. Here, δ is the delta function, n_m is the modified index of refraction, and n_g is complex index of refraction of the earth.

At sufficiently large distances above and below the earth's surface, $\Pi(ks,z)$ must be an outgoing wave whose phase has a negative imaginary part. Let the solution to

$$\left[\frac{d^2}{dz^2} + k^2 n_m^2\right]u(z) = 0 \tag{42}$$

that satisfies the boundary conditions for $z>z'$ be equal to $A\ u_1(z)$, and the solution to this equation for $0<z<z'$ be equal to $B\ u_1 + C\ u_2$, where u_2 is a second linearly independent solution and A, B, and C are constants. The solution below the earth's surface is given by

$$D \exp\left[jk(n_g^2 - s^2)^{1/2}z\right] \quad , \tag{43}$$

where the branch of the square root is chosen such that the imaginary part of $(n_g^2 - s^2)^{1/2}$ is less than zero and D is another constant. z is chosen to be negative below the earth's surface.

Because we are interested only in the fields above the earth surface, it suffices to satisfy the boundary condition

$$\frac{\partial\Pi(ks,z)}{\partial z}\left[\frac{1}{\Pi}\right] = p \quad , \tag{44}$$

where

$$p = jk\left(n_g^2 - s^2\right)^{1/2} \tag{45}$$

for horizontal polarization and

$$p = jk\frac{n_m^2}{n_g^2}\left(n_g^2 - s^2\right)^{1/2} \tag{46}$$

for vertical polarization (Fishback, 1964). In addition, equation (40) requires that the discontinuity in the derivative of $\Pi(ks,z)$ with respect to z evaluated at z' be equal to -1; and that $\Pi(ks,z)$ be continuous at $z = z'$.

Using these constraints we obtain for z greater than zero

$$\Pi(\rho,z) = \frac{k^2}{4\pi}\int_{-\infty}^{\infty}\frac{H_0^{(2)}(ks\rho)}{W}u_1(z_>)y_2(z_<)sds\ , \tag{47}$$

where $z_>(z_<)$ stands for the greater (smaller) of z and z', and y_2 is given by

$$y_2(z) = u_2(z) + \left[\frac{u_2(0)p - u'_2(0)}{u'_1(0) - pu_1(0)}\right]u_1(z)\ . \tag{48}$$

Here, u'(0) indicates that u is differentiated with respect to z and evaluated at z equal to zero, and W is the Wronskian of u_1 and u_2 evaluated at $z = z'$. The Wronskian is explicitly given by

$$W = u'_2u_1 - u'_1u_2\ . \tag{49}$$

The Wronskian of equation (42) is a constant, independent of z.

The contour of integration for $\Pi(\rho,z)$ is along the real axis. Because of the asymptotic properties of the Hankel function, this integral is equal to the sum of the poles and the integration around the branch cut in the lower half-plane (Baumgartner, 1983). The integration around the branch cut is

associated with the surface wave and will be neglected. The poles are located where

$$u'_1(0,s) - p(s)u_1(0,s) = 0. \tag{50}$$

The expression determines the eigenvalues s_N. Hence, neglecting the surface wave we have

$$\Pi(\rho,z) = -\frac{jk^2}{2} \Sigma \frac{H_0^{(2)}(ks_N\rho)s_N u_1(z_>)u_1(z_<)[u_2(0)p - u'_2(0)]}{W \frac{d}{ds}[u'_1(0) - pu_1(0)]} , \tag{51}$$

where the sum is performed over the eigenvalues s_N. This result can be written as

$$\Pi(\rho,z) = -\frac{j}{2} \Sigma \lambda_N E_N(z,z')H_0^{(2)}(ks_N\rho)(ks_N)^{1/2}s_N , \tag{52}$$

where λ_N is given by

$$\lambda_N = \frac{k2(ks_N)^{1/2}}{W\frac{d}{ds}[u'_1(0) - pu_1(0)]} \tag{53}$$

and E_N is given by

$$E_N(z,z') = u_1(z_>)u_1(s_<) . \tag{54}$$

λ_N and E_N are referred to as the modal excitation factor and the modal height-gain function (Baumgartner, 1983).

For arbitrary refractivity profiles, the solutions u_1 and u_2 are not generally available. In any region where the modified refractive index can be treated as locally linear, the Airy functions Ai and Bi are linearly independent solutions to equation (42). The rate of change of the modified index of refraction is on the order of one over the earth's radius; hence, for distances on the order of a wavelength in the LoVHF band, the modified index

of refraction changes very little. Consequently, in a region which is far from a zero of $q^2 = n_m^2 - s^2$, WKB solutions can be used to describe u_1 and u_2. Assuming that s_N is real in regions where q^2 is less than zero, Π decreases with height; and in regions where q^2 is greater than zero, Π is oscillatory. Hence, if the zeros of q are sufficiently isolated, the effect of the layers above the reflection level on the value of Π below the reflection level is minimal. The situation is similar to the case where the modified index of refraction continues to decrease for all heights above the reflection level. Furthermore, if the zeros of q are isolated, then the medium must be locally linear. Consequently, if the zeros of q are sufficiently isolated, the Airy function Ai is an adequate solution in the neighborhood of the reflection level, and at heights below the reflection level the solutions are reasonably approximated by the WKB solutions. In this case, the reflection coefficient reference to the level of reflection is equal to $\exp(j\frac{1}{2}\pi)$; and, for distances sufficiently below the reflection level, u_1 is given by

$$u_1(z) \quad \frac{1}{\sqrt{q}}\left[\exp\left(-jk\int_{z'}^{z} q\,dz\right) + j\,\exp\left(-jk\int_{z'}^{z_0} q\,dz\right)\,\exp\left(-jk\int_{z}^{z_0} q\,dz\right)\right] , \qquad (55)$$

where z_0 is the reflection height. Here, the first term represents an upgoing wave and the second a downgoing wave that has been reflected at the height z_0. In this case, it is easy to show that the poles are located where

$$1 - R_G R_T = 0 , \qquad (56)$$

where R_G is the Fresnel reflection coefficient of the earth, and R_T is the reflection coefficient of the troposphere referenced to the ground, here given by

$$R_T = j\,\exp\left(-2jk\int_{0}^{z_0} q\,dz\right) . \qquad (57)$$

If $|ks\rho|$ is much greater than one, $H_0^{(2)}$ is proportional to $\exp(-jks\rho)$; hence, the modal functions can be thought of as cylindrical waves with local wave vectors $k(s\rho + qz)$, where ρ and z are unit vectors in the ρ and z directions, respectively. If we let $s = \sin(\phi)$, then equation (56) defines a discrete set of generally complex eigenangles.

This description of the problem will generally be accurate everywhere except where the reflection level is near a minimum of n_m. In these regions the modal functions and the eigenvalues may not be well described by this formalism. In order to obtain a more accurate description, the exact solutions may have to be used.

For simplicity let us consider the case of horizontal polarization. In the LoVHF band, R_G is then approximately equal to -1. In this case the eigenangles are defined by

$$\int_0^{z_0} q\,dz = \frac{\lambda}{2}(m - 1/4) \ , \tag{58}$$

where m is an integer greater than one (Budden, 1961a, Booker and Walkinshaw, 1946). Note that this expression determines the eigenangles as a function of the medium below the reflection level only. This result is in agreement with our earlier comments on the effects of the medium above the reflection level; however, in general, the eigenangles will be affected by the characteristics of the medium at all levels.

If the mode number m or the wavelength λ increases, the left-hand side of this expression must also increase. This is generally accomplished by increasing the height of reflection and decreasing the magnitude of s. This implies that larger values of m or λ correspond to cylindrical waves with larger elevation angles. Suppose that n_m^2 achieves its minimum value of n_{min}^2

at a height of z_{min}; then if s^2 is greater than N^2_{min}, z_0 and s must both be complex. So as the mode number increases, the eigenangles eventually become complex. This leads to a situation where the modes are leaky (Budden, 1961a). If $s = N_{min}$, $z_0 = z_{min}$, and the left-hand side of equation (58) is less than $3\lambda/8$, then all the modes are leaky. This condition is often used to determine a measure of the minimum frequency which is trapped by the duct. The larger the wavelength λ, the smaller the number of trapped modes. For frequencies in the LoVHF band, one mode is generally sufficient to describe the ducted field (Pappert and Goodhart, 1977).

If n^2_m increases with height, as it does for zero duct height, the eigenvalues are all complex and the modes decay with increasing height and distance along the earth's surface (Budden, 1961a). This is the prevailing picture when diffraction is the dominant effect. Hence, for a sufficiently large distance from the transmitter, one mode is adequate to describe the diffracted field (Fishback, 1964, Hitney et al., 1984).

The program XWVG (Baumgartner et al., 1983) uses a trilinear model for the tropospheric modified index of refraction. For the trilinear model the modified index of refraction n_m initially increases linearly as the height above the earth's surface increases; eventually a height is reached where n_m begins to linearly decrease with increasing height; and finally, at a height where n_m takes on its minimum value, it increases linearly for all greater heights. For a trilinear model two linearly independent solutions to equation (42) are the Airy functions Ai and Bi. XWVG uses these exact solutions throughout its calculations.

XWVG is intended for use over the sea and does attempt to include the effect of surface roughness. The program could be easily extended for use over land by including the dielectric constants for the ground. For ranges

much greater than a few wavelengths from the receiver, the Hankel function $H_0^{(2)}$ is proportional to exp(-jksρ). XWVG uses the Shellman-Morfitt root-finding technique to determine the eigenvalues (Baumgartner et al., 1983). As the mode number increases, the magnitude of s increases. When exp(-kρIm[s]) decays more rapidly than a specified rate, the program ceases to calculate modes (usually at about 1 dB/km). Here, Im[s] means the imaginary part of s. Baumgartner et al. (1983a) have also investigated the possibility of using the asymptotic expansions of the Airy functions to decrease the processing time of the XWVG program. They found that while computation time was reduced by about one-twentieth, accuracy was not significantly affected (Baumgartner et al., 1983a).

The method used by IREPS for calculating the ducted and diffracted fields is considerably simpler than the methods of XWVG. For the diffracted field and the field due to evaporation ducts (weak, shallow ducts produced over water), IREPS uses a single-mode approximation. This mode is calculated for a frequency of 9.6 GHz. The height-gain function and excitation factors at other frequencies are obtained by the use of scaled ranges and duct heights (Hitney et al., 1984). IREPS apparently assumes an earth reflection coefficient of -1, an approximation valid for horizontal polarization but not adequate, in the LoVHF band, for vertical polarization. Generally, evaporation ducts are of no importance for the LoVHF band (Hitney et al., 1985); however, this portion of IREPS might still be of value in the calculation of the diffracted field.

Surface-based ducts of sufficient thickness can be important in the LoVHF band. IREPS uses an empirical fit to data to determine the height-gain function for these ducts (Hitney et al., 1984). Since IREPS is designed to

work in the HiVHF band, it is uncertain how well these models would work in the LoVHF band.

4.2 CONCLUSION FOR RANGES LESS THAN 500 km

The method that we recommend for distances less than 500 km would be the following. Within the line-of-sight distance use EPM-73, Longley-Rice, or a version of IREPS modified to include reflection from the ground. EPM-73 is the crudest, but simplest, of these models. Longley-Rice is more complicated but provides for a greater variety of situations. SRICOM includes both models and, therefore, provides for the advantages of both. IREPS is primarily intended for use over seawater but could be modified for propagation over land. The complexity of the IREPS model lies somewhere between that of EPM-73 and the Longley-Rice models.

For distances beyond line of sight, obtain by statistical or experimental means a model of the tropospheric index of refraction. Then use the program XWVG or a simplified version of this program to calculate the field strength. For distances sufficiently far from the radio horizon, a single mode will be adequate to describe the field in the LoVHF band. In the intermediate region use the method of "bold interpolation" to determine the field strength. In this manner, both the diffracted and ducted fields are calculated simultaneously. The losses due to tropospheric scattering can be continually calculated using methods employed in the Longley-Rice, EPM-73, or IREPS models. When the loss due to tropospheric scattering is less than that due to ducting or diffraction, tropospheric scattering is assumed to dominate the behavior of the fields and, for greater distances, only the loss due to tropospheric scattering is calculated. This manner of treating tropospheric scattering is the method used by IREPS (Hitney et al., 1984). It is possible,

however, that the ducted fields will always be larger than the fields scattered from the troposphere. In fact, ducting may be important for ranges beyond 500 km. We will deal with this possibility in the next section.

4.3 RANGES BEYOND 500 km

At distances beyond 500 km, propagation via the ionosphere becomes the dominant mode. For frequencies less than the classical MUF, refraction is the dominant means of propagation. At the classical MUF the receiver is located on the edge of the skip zone. However, because of the existence of other modes of propagation, for frequencies beyond the classical MUF the field strength does not abruptly fall to zero. For this reason it is difficult to determine the value of the classical MUF. Instead the MUF is often determined by combining data obtained from vertical soundings of the ionosphere with a model of ray propagation through the ionosphere. When the MUF is obtained in this way it is referred to as the standard MUF. The standard MUF is considered to be a reasonable approximation to the classical MUF (Davies, 1965). Unless specifically indicated, we will refer to both the classical and standard MUF's as simply the MUF.

For frequencies above the MUF, propagation by refraction alone is no longer possible. Among the causes of propagation beyond the MUF are (i) ionospheric scattering, (ii) transequatorial propagation, (iii) side scatter due to ground irregularities, (iv) sporadic E layer propagation, and (v) off-great-circle propagation by horizontal gradients of ionization rays (Damboldt, 1976, Beckmann, 1965). For frequencies less than the MUF, analytical means exist for calculating the field strength; however, for frequencies greater than the MUF and less than the MOF, attempts to explicitly calculate the influence of each of the physical processes involved have not

been successful (Damboldt, 1976). For this reason the effects of over-the-MUF propagation modes are usually taken into account on a statistical and empirical basis.

In order to use analytical methods to calculate the field strength for frequencies less than the MUF, a description of the state of the ionosphere must be obtained. In general, because of lateral variation in the ionosphere, the state of the ionosphere must be described at more than one point along the path of the ray. The points along which the ionosphere is described are called control points. Generally, the state of the ionosphere near the midpoint of each hop is desired. However, for short path lengths involving multiple hops, the ionosphere is reasonably homogeneous over the range of propagation, and for long path lengths, the number of calculations can become excessive. For this reason most models limit the number of calculations for long ranges and make only one calculation at the midpoint for sufficiently short ranges.

Over the path of each hop the ionosphere is generally assumed to be spherically stratified and laterally homogeneous. In the LoVHF band reflections from the normal E layer are not possible. However, the E layer can produce retardation effects that will have an effect on the field strength. The D layer has no refractive effect on the ray, but significant absorption takes place in the D layer. In general, a model of the entire ionosphere is necessary to characterize its effects on the field strength.

If a parabolic model is used to approximate the electron density in the F layer, the electron density can be described in terms of the maximum plasma frequency foF2 and the heights at the bottom and the peak of the layer. The

collection of large amounts of ionospheric data has made it possible to describe the global state of the ionosphere with reasonable accuracy. A description of the monthly median values of foF2 can be expressed as a Fourier diurnal time series (CCIR Report 340, Oslo, 1966). The coefficients, given at either a sunspot number of 0 or 100, are functions of the geographical location and season. The coefficients at other sunspot numbers are obtained by linear interpolation. A simplified method of expressing these data is presented by Rose et al. (1978). Similar expansions exist for the ratio of the MUF to foF2 at 3000 km due to propagation through the F2 layer, M(3000)F2 (CCIR Report, 340, Oslo, 1966), for ratios of the peak of the F2 layer to the half-thickness of the F2 layer (Lucas and Haydon, 1966), the critical frequency of the F1 layer (foF1) (Rosich and Jones, 1973), and for the maximum plasma frequency in the E layer (foE) (Leftin, 1976). From the values of M(3000)F2 it is possible to predict the value of the peak of the F2 layer (Skimazaki, 1955). The peak of the F1 layer is primarily a function of the solar zenith angle χ and is approximately given by $165 + 0.6428\chi$, where the height is given in km (Lloyd et al., 1978). The E layer is generally modeled as a parabolic layer with an assumed peak height and half-thickness. Commonly, the height of the peak is set at 110 km and the half-peak at 20 km (Lloyd et al., 1978, CCIR Report 252-2, 1970, Lucas and Haydon, 1966). Finally, it is possible to describe the D layer by an exponential decay of electron density with decreasing height (Lloyd et al., 1978). Most models explicitly include descriptions of only the E and F2 layers (CCIR Report 252-2, 1970, Lucas and Haydon, 1966). However, IONCAP (Lloyd et al., 1978) includes descriptions of the D, E, F1, and F2 layers in its model of the ionosphere.

Given a description of the ionosphere, it is possible to determine the range as a function of the angle which the ray makes with the vertical. At the skip zone the rate of change of the range with angle is zero. The frequency at which the skip zone is located at the distance to the receiver is the MUF. This is the method used by Appleton and Beynon (1947) and the CCIR Report 252-2 (1970). Though this method can, in principle, be applied for any ionospheric model, it is not the method commonly used to determine the MUF. The methods commonly employed rely on numerical fits to the results of more careful analysis (Lockwood, 1983, Rose et al., 1978, Lloyd et al., 1978). All of these methods neglect the effect of the earth's magnetic field on the path of the ray. The X wave has a higher MUF associated with it than the O wave (Davies, 1965). For quasi-longitudinal propagation, the separation between these MUFs is equal to the electron gyromagnetic frequency f_H (Davies, 1965). A common method of accounting for this difference is to add $\frac{1}{2}f_H$ to the MUF calculated on the basis of there being no magnetic field (Lloyd et al., 1978).

Given a model for the variation of the electron density N, the signal strength can in principle be calculated. For frequencies in the LoVHF band, the effect of the earth's magnetic field can generally be neglected in the calculation of the field strength. The index of refraction n is then given by

$$n^2 = 1 - \frac{f_p^2}{f^2}, \tag{59}$$

where f_p is the plasma frequency and is a function of position (Budden, 1961b). In the geometrical optics approximation the field strength of an isotropic radiator is given by

$$\left(\frac{P_T Z_0}{4\pi}\right)^{1/2} \frac{1}{S_E}, \tag{60}$$

where P_T is the transmitter power, and Z_0 is the impedance of free space. s_E is the distance that the field would have to propagate in free space to achieve the same field strength. For a spherically symmetric ionosphere

$$s_E^2 = \alpha \sin(\phi) \tan(\phi_0) \frac{\partial D}{\partial \phi_0} , \tag{61}$$

where α is the earth's radius, ϕ is the angle subtended from the center of the earth over the range D of propagation, and ϕ_0 is the angle which the ray makes with the normal to the earth's surface. $\partial D/(\partial \phi_0)$ is to be evaluated for a given range D, with the relationship between D and ϕ_0 defined by

$$D = 2a^2 \sin(\phi_0) \int_{\alpha}^{r_0} \frac{dr/r}{\left\{n^2 r^2 - [\alpha \sin(\phi_0)]^2\right\}^{1/2}} . \tag{62}$$

Here, r_0 is the reflection level of the ray and is defined by

$$n^2(r_0) r_0^2 = [\alpha \sin(\phi_0)]^2 . \tag{63}$$

Bibl et al. (1952) make use of this method in calculating the field strength. They assume that both the E and F layers are well modeled by a parabolic layer. Using equation (62), they solve for $\sin(\phi_0)$ for a fixed value of D and then use this result in the expression for s_E.

However, most models do not use this method of calculating the field strength. This method requires a relatively simple model for the electron density in order to be able to integrate equation (62) for D, and once integrated, it is difficult to invert the result to find ϕ_0. Furthermore, the expression for the effective distance of propagation SE is invalid for frequencies near the classical MUF, where $\partial D/(\partial \phi_0)$ tends to zero, and for small elevation angles, where $\tan(\partial_0)$ tends to zero. The method used by most models is to neglect the focusing effect in these regions and to find, instead, a measure of path length along the ray. The advantage of this method

is that it is always nonzero and reduces to the correct expression in free space.

The measure that is most commonly used is the group path h_G along the ray. For a spherically symmetric ionosphere we have

$$h_G = \int_{\alpha}^{r} \frac{r dr}{\{n^2 r^2 - [\alpha \sin(\phi_0)]^2\}^{1/2}} \quad . \tag{64}$$

Note that in free space h_G is equal to the distance of propagation along a straight ray. For a given time of propagation, the group path h_G is the equivalent distance that a pulse would travel in free space. The group path is a positive definite quantity which tends to infinity only as the time of propagation tends to infinity. Hence, characteristics of the group path are similar to those of the distance of propagation in free space. The group path has the further advantage, as we shall soon see, of being somewhat related to the equivalent height of reflection h_v. The equivalent height of reflection is the height at which a vertically incident wave would be reflected from the ionosphere were it travelling in free space. This is exactly the kind of information that an ionsonde provides.

For a flat earth the group path is equal to

$$h_G = \int_{0}^{z} \frac{dz}{\left[n^2(z) - \sin^2(\phi_0)\right]^{1/2}} \quad , \tag{65}$$

where z is the height above the earth's surface. For a transmitter and receiver separated by a distance R and transmitting at a frequency fob, by Breit and Tuve's theorem

$$h_G = \frac{R}{\sin(\phi_0)} \quad , \tag{66}$$

and by Martyn's theorem

$$h_G(\text{fob}) = 2 \sec(\phi_0) h_v(f\nu) \ , \tag{67}$$

where

$$\text{fob} = f\nu \sec(\phi_0) \ , \tag{68}$$

and h_v is the equivalent height of reflection. Using Breit and Tuve's and Martyn's theorems, we find that the equivalent height of reflection of the oblique ray is $h_v(f\nu)$. The result of this analysis shows that a wave transmitted at a frequency fob in free space and specularly reflected at a height $h_v(f\nu)$ on its way to a ground-based receiver will have the same group path as the wave transmitted under identical conditions through the ionosphere.

Using equations (66) through (68), we obtain

$$h_v(f\nu) = \frac{1}{2} R \left[\left(\frac{\text{fob}}{f\nu} \right)^2 - 1 \right]^{1/2} \tag{69}$$

$$\tan(\phi_0) = \left[\left(\frac{\text{fob}}{f\nu} \right)^2 - 1 \right]^{1/2} \tag{70}$$

$$h_G(\text{fob}) = \frac{1}{2} R \frac{1}{\left[\left(\frac{\text{fob}}{f\nu} \right)^2 - 1 \right]^{1/2}} \tag{71}$$

h_v as a function of frequency can be obtained either from an ionogram or by integration of equation (65) with ϕ_0 equal to zero. Then, by either graphical or analytical methods equation (69) can be solved for $f\nu$ as a function of R and fob. With this solution equations (70) and (71) can be used to find the take-off angle ϕ_0 and the group path h_G.

The flat earth approximation is valid if the bulge of the earth is much less than the effective height of reflection, and the range R is much less than the earth's radius. The range beyond which the curvature of the earth must be taken into account is typically set at about 500 km (Davies, 1969).

The situation for a curved earth is considerably more complicated than for a flat earth. In analogy with the flat earth result, a vertical frequency $f\nu$ is defined such that both the oblique and vertically incident rays reflect at the same height. With this definition, we obtain

$$f\nu = \text{fob}[1 - n^2(r_0)]^{1/2} , \tag{72}$$

where r_0 is the level of reflection and is defined by equation (63). In principle, it is possible to solve for ϕ_0 for a given range D and then use that result in h_G. This is essentially the method used by Kobayashi (1961). He was able to approximate the equation for D and h_G in terms of $h_v(f\nu)$, the level of reflection r_0, and d_0. Given a model of the electron density, it is then possible to derive the functional forms of $h_v(f\nu)$ and r_0 and, then, to obtain ϕ_0 and $h_G(\text{fob})$ for a given range D. Because this method is complicated, simpler approaches have been sought.

A simpler method was proposed by Smith (1939). If over the distance which the ray propagates through the ionosphere, the ionosphere can be considered flat, then for that portion of the path in the ionosphere both Breit and Tuve's and Martyn's theorems are applicable. This means that both the horizontal and vertical penetrations of the ray into the ionosphere must be small compared with earth's radius. Over the distance of propagation below the ionosphere, the rays are straight, and the group path can be easily calculated.

Let ϕ equal the angle which the ray in free space makes with the radial vector at the virtual height of reflection of the oblique ray. Then we have

$$\tfrac{1}{2}h_G(\text{fob}) = (a + h_0)|1 - 2(h_v - h_0)\sin^2(\phi)|^{1/2}$$

$$- [a^2 - (a + h_v)^2 \sin^2(\phi)]^{1/2}$$

$$+ \frac{h_v - h_0}{a + h_0} \left[\frac{1}{1 - 2(h_v - h_0)\sin^2(\phi)} \right]^{1/2} \tag{73}$$

$$f\nu = \text{fob} \cos(\phi) \left[1 - 2\frac{h_v - h_0}{a + h_0} \tan^2(\phi) \right]^{1/2} \tag{74}$$

$$\tan(\phi) = \frac{\sin(R/2\alpha)}{1 + h_v/\alpha - \cos(R/2\alpha)} \ . \tag{75}$$

Here, h_0 is the height of the base of the ionosphere, R is the range, α is the radius of the earth, and h_v is evaluated at a frequency of $f\nu$. Using equations (74) and (75) it is possible to solve for ϕ and $f\nu$ as functions of R and fob. These results can then be used in equation (73) for h_G. This is the method used by Lucas and Haydon (1966). In this curved earth and flat ionosphere approximation, as in the flat earth approximation, the virtual height of reflection of the oblique ray is equal to $h_v(f\nu)$.

For longer ranges and deeper penetrations into the ionosphere, the ionosphere can no longer be treated as flat. One approach is to simply assume that the equivalent path in free space is equal to the group path and that the virtual height of reflection is equal to $h_v(f\nu)$. In this case

$$\frac{1}{2}h_G(\text{fob}) = \frac{\alpha \sin(R/2\alpha)}{\sin(\phi)} \ . \tag{76}$$

$f\nu$ is given by equation (74), with h_0 replaced by the level of reflection hr = $r_0 - \alpha$, and $\tan(\phi)$ is given by equation (75). This is the method used by the CCIR (CCIR Report 252-2, 1970). They are able to integrate the integral for h_v by assuming parabolas for both the E and F layers.

However, the assumptions of this method are highly suspect (Smith, 1939). IONCAP (Lloyd et al., 1978) recognizes this difficulty and adjusts the virtual height of reflection of the oblique ray by adding to $h_v(f\nu)$ the quantity

$$\left\{\frac{fob^2 - fv^2}{fobF2^2}\left[\frac{h_r}{\alpha}(h_v - h_r) + 2(\alpha + h_r)\left(\frac{h_v - h_r}{\alpha}\right)^2\right]\right\} \quad , \tag{77}$$

where foF2 is the maximum plasma frequency and h_v is evaluated at a frequency of fv. Note that if $(h_v - h_r)/\alpha$ is much less than one, equation (77) is small. This is essentially the assumption of the flat ionosphere and curved earth model. Because IONCAP (Lloyd et al., 1978) uses a rather complicated, albeit realistic, model of the electron density they must use numerical integration to obtain values of $h_v(fv)$.

A later CCIR model (CCIR, 1984) expresses the virtual height of reflection of the oblique ray as a simple function of foF2/foE, the range, and M(3000)F2. This functional form is based upon an extensive study of ray propagation in a quasi-parabolic layer. The results are believed to be accurate to within 10% for frequencies greater than twice foE and for values of the M factor (f/MUF) in the range 0.8 to 0.95 (Lockwood, 1984). In the LoVHF band the frequency will commonly be near the MUF; consequently, we can expect this expression for the virtual height of reflection to be reasonably accurate.

Having determined the virtual height of reflection using either the method proposed by the CCIR or IONCAP, the group path can then be determined by the use of equations (75) and (76), with $h_v(fv)$ replaced by the corrected values of the virtual height of reflection.

The loss of power or field strength due to path length is commonly referred to as the free space loss, L_{fs}. In addition, the effects of deviative, nondeviative, and auroral absorption, ground losses, off-great-circle paths, sporadic E, and scattering must also be taken into account.

Usually, for frequencies less than the MUF, the most important loss after the free space loss is due to ionospheric absorption. Nondeviative absorp-

tion takes place in the D and E layer and is proportional to f^{-2} (Davies, 1965). Deviative absorption takes place near the level of reflection and has a complicated frequency dependence (Davies, 1965). It is particularly large when the reflection level is near a maxima of the electron density, as it is for a Pedersen ray. If initially only nondeviative absorption is considered, the absorption loss due to absorption in dB L_i is as given by (Davies, 1965):

$$L_i = \frac{2.17}{(2\pi)^2 c} \int_0^z \frac{f_p^2 \nu \sec(\phi_0)}{(f + f_H)^2 + (\nu/2\pi)^2} dz \quad . \tag{78}$$

Here, f_p is the plasma frequency, ν is the collision frequency, c is the speed of light, ϕ_0 is the angle which the ray makes with the vertical, f_H is the electron gyrofrequency, and f is the frequency. The plasma frequency f_p is equal to $N(z)e^2/(m\varepsilon_0)$, where N is the electron density, e the charge of an electron, m the mass of an electron, and ε_0 the dielectric constant of free space. Equation (78) is obtained on the basis of quasi-longitudinal propagation of the ordinary wave through a horizontally stratified ionosphere. As such, it neglects ionosphere curvature. This is an adequate approximation if the distance over which the major contribution to the integral accrues is sufficiently small. In a typical ionosphere, as the height z decreases, f_p decreases and increases. The net effect is that nondeviative absorption is most important in the D and E layers. The electron concentration and collision frequency are complicated functions of the solar zenith angle, season, geographical location, and sunspot number.

Those rays which are generally most important to the determination of the field strength do not reflect at heights near the peak of the F layer. We would therefore expect the absorption loss L_i due to both deviative and nondeviative absorption to take a functional form similar to that given by deviative absorption alone. A semiempirical model of the total ionospheric

absorption loss, based upon data derived from F layer propagation, has been developed by Lucas and Haydon (1966):

$$L_i = \sum_{j=1}^{n} \frac{677.2n \sec(\phi_0) I}{(f + f_H)^{1.98} + 10.2} + Y_p \qquad (79)$$

$$I = (1 + 0.0037R_{12})[\cos(0.881\chi_j)]^{1.3} , \qquad (79a)$$

where n is the number of hops, χ_j is the solar zenith angle for the j^{th} hop, R_{12} is the sunspot number, and Y_p is a geographical and seasonal correction factor. This is the model used by the CCIR (CCIR Report 252-2, 1970, CCIR, 1984). IONCAP uses a different expression for I that is based on the relationship between I and foE; namely,

$$I = -0.04 + \exp(-2.937 + 0.8445 foE) \qquad (79b)$$

(Lloyd et al., 1978). The factor 10.2 in the denominator of equation (79) has been included to account for tne low-frequency dependence of L_i when $(f + f_H)$ approaches $\nu/(2\pi)$. It can be neglected for frequencies in the LoVHF band. At night the absorption changes little with time; consequently, the value of I is constrained to be above 0.1 (Lucas and Haydon, 1966). The correction factor Y_p is an empirically determined quantity which takes into account geographic and seasonal variations in absorption not included in the first expression on the right-hand side of equation (79). These quantities are largest during the morning hours of equinoctal periods at geographic latitudes near 65 deg (Lucas and Haydon, 1966). This is exactly the time when auroral absorption is largest (Davies, 1965). To a considerable extent, then, Y_p is an attempt to include the effect of auroral absorption.

Equation (78) for L_i was derived from an average of F2 propagation data for frequencies less than the FOT (90% of MUF) and for ranges from 55 to 15,000 km (Laitinen and Haydon, 1962, Lloyd et al., 1978). The overwhelming

majority of these data were derived from ray trajectories with low elevation angles and ranges less than 7000 km (Laitinen and Haydon, 1962). Since L_i was intended to represent ionospheric absorption, ground losses L_G were subtracted out (Laitinen and Haydon, 1966). Y_p was derived from the same data set used in deriving the first expression on the right-hand side of equation (78) (Lucas and Haydon, 1966) and, consequently, is applicable for the same ray set. If more than one set of ray trajectories is included in the field strength calculation, Y_p should be added to the total loss formula only once. This is so because the derivation of Y_p makes no distinction between different modes of propagation.

Equation (78) takes into account the average effect of passage through the D and E layers and the lower regions of the F layer. It therefore accounts for nondeviative losses, low-angle deviative losses, auroral absorption (in Y_p), and possibly some losses due to transmittance through sporadic E layers. It does not effectively take into account losses for frequencies greater than the FOT, ranges greater than about 7000 km, ground losses, and deviative losses for rays which reflect from heights close to the peak of the E and F layers. It overestimates the losses for those rays which are reflected from sporadic E layers and does not include reflection losses from sporadic E layers. Even though some sporadic E transmission losses may be included in L_i, the averaging process would probably make it necessary for a given mode to take these losses explicitly into account. IONCAP (Lloyd et al., 1978) attempts to adjust L_i for those cases when the ray either does not reach the F layer or reflects close to the peak of the F layer. For the LoVHF band neither of these cases is particularly important, since E layer reflection is not possible and rays that reflect near the peak of the F layer tend to be so attenuated as to not be the dominant mode of propagation.

Consequently, the additional losses that need to be considered are (i) ground losses L_G, (ii) losses due to sporadic E, and (iii) losses associated with frequencies greater than the FOT.

Ground losses are taken into account by both CCIR models (CCIR Report 252-2, 1970, CCIR 1984), Lucas and Haydon (1966), and IONCAP (Lloyd et al., 1978). The early CCIR model (CCIR Report 252-2, 1970) uses the same method employed by Lucas and Haydon (1966). The later CCIR model (CCIR, 1984) simply subtracts 2 dB per hop.

Off-great-circle paths are due to the lateral inhomogeneity of the ionosphere. The average global characteristics of the ionosphere are laterally inhomogeneous. Calculations made by Kovalevshayi and Kornitskaya (1969) indicate that these gradients in the ionosphere can result in an angle of arrival that deviates by as much as 5 deg from the great circle path and can increase the MUF by as much as 35%. However, a 5-deg variation from the great circle path will increase the path length by less than about 0.5%. Consequently, though the lateral inhomogeneities are apparently important in the prediction of the MUF, they have little effect upon the field strength.

Below the MUF scattering is relatively unimportant because it is a comparatively weak mode, whereas above the MUF it may be the only mode available. Above-the-MUF losses are dealt with on a statistical basis and will be discussed later.

In the LoVHF band reflection from the normal E layer is not possible. However, under sporadic E conditions the E layer can have significant effects upon the signal strength. Sporadic E layers produce two important effects. They reflect waves which normally would not be reflected, and they attenuate waves which are transmitted through them. In general, both reflection and transmission (obscuration) losses must be accounted for (Sinno et al., 1976).

To calculate the losses due to the sporadic E layers, rays could be traced through the ionosphere with the layers present. Reflections from the sporadic E layers would incorporate losses due to those reflections, and those rays which pass through the sporadic E layers would incorporate obscuration losses. This is the method used by IONCAP (Lloyd et al., 1978). Generally, due to substantial absorption losses in the D layer, those modes which have greater than two reflections from the sporadic E layers can be neglected (CCIR, 1984). In those cases where no F layer mode exists, reflection from the E layer is the only possible reflection mechanism. This situation prevails when the frequency is greater than the classical MUF and for ranges less than about 2000 km. For frequencies above the MUF, sporadic E propagation produces a maximum field strength at distances of 1500 km (Miya and Sasaki, 1966) and can generally be neglected for ranges greater than 4000 km (CCIR, 1984).

The calculation of the field strength produced by sporadic E layer propagation must be statistical in nature, because prior knowledge of the existence of these layers is not readily available. Miya and Sasaki (1966) relate the probability of the loss Γ due to reflection from sporadic E layers being less than a given value and the equal probability of the maximum plasma frequency of the sporadic E layer, foEs, exceeding a given value. This loss Γ is intended to not include free space losses, ionospheric absorption losses, and ground losses (Miya et al., 1978). Using global data on the probability of foEs exceeding 7 MHz, it is possible to use the Phillips rule and determine the probability of foEs exceeding a frequency f (Smith, 1976, CCIR Recommendation 534, 1978). The method presented by Miya and Sasaki (1966) and Miya et al. (1978) for the calculation of sporadic E field strengths is essentially the method recommended by the CCIR (CCIR Recommendation 534, 1978,

CCIR Recommendation M534-1, 1982). Because obscuration losses are neglected, this model is valid only for frequencies greater than the classical MUF.

Sinno et al. (1976) have attempted to measure the reflection and transmission coefficients through sporadic E layers. Under sporadic E conditions, the trace on an ionogram due to reflection from the F layer is not visible for frequencies less than the blanketing frequency fbEs. For frequencies above foEs, there is no E layer trace. Hence, for frequencies less than fbEs, the transmission coefficient is near zero, and for frequencies above foEs, the reflection coefficient is near zero. For thin layers Breit and Tuve's and Martyn's theorems are applicable within the layer (Smith, 1939). In this case the group path for vertical incidence at a frequency fυ is related to the group path at oblique incidence at a frequency fob = $f\nu \sec(\phi)$, where ϕ is the angle which the ray makes with the radial vector at the bottom of the layer. Hence, these conclusions about the reflection and transmission coefficients at vertical incidence are equally true at the equivalent oblique frequency fob. We, therefore, expect the reflection and transmission coefficients to be functions of $f\nu$.

Sinno et al. (1976) find that the reflection losses at the frequencies foEs and fbEs are about 20 and 0.7 dB, respectively. Consequently, the reflection loss, R, (in dB) is approximately given by

$$R = -20 \log(r) = 20 \log[1 + 10(f\nu/foEs)^m] , \qquad (80)$$

where r is the reflection coefficient. The transmission coefficient t is given by

$$t = [1 - r^2] . \qquad (81)$$

Given the value of fbEs, the value of m can be determined, assuming that R = 0.7. If the value of fbEs is unavailable, Sinno et al. (1976) suggest that a

value of 8 for m is generally satisfactory. If the median values of foEs and fbEs are known, it is possible to calculate the median field strength by tracing rays through the ionosphere, taking into account reflections from both the E and F layers. The group path due to reflection from a sporadic E layer can be calculated on the basis of a thin layer, and losses due to passing through and reflecting from the sporadic E layer can be calculated using equations (80) and (81). Furthermore, equation (80) for R appears to be adequate even if instantaneous values of foEs are used (Sinno et al., 1976). Consequently, if equation (80) is viewed as a functional relationship between the reflection coefficient, foEs, and fbEs, it would be possible, given the probability distribution of foEs and foEb, to calculate the probability of a given signal strength.

Another method of calculating the effects of the sporadic E layer is used in IONCAP. The method is based upon the Phillips-Abel theory (Wheeler, 1966). This theory is based upon the observation that the temporal probability of occurrences of foEs is proportional, if not equal, to the spatial probability of occurrence of foEs (Phillips, 1963).

For a vertically incident ray, if the frequency f_v is less than foEs, the ray will be reflected. For oblique incidence we require that fob be less than the vertical frequency f_v, foEs sec(ϕ), if reflection is to take place, where ϕ is the angle which the ray makes with the radial direction at the bottom of the sporadic E layer. The greater the number of such reflecting regions, the greater will be the reflected signal strength. Hence, the power reflected from a sporadic E layer must be proportional to the probability P that foEs sec(ϕ) is greater than fob, and the loss R in decibels is proportional to 10 log(P).

The probability of foEs exceeding a particular value can be obtained by using the Phillips rule (Phillips, 1963, Smith, 1976),

$$\log \frac{P_1}{P_2} = b[f_1 - f_2] \ . \tag{82}$$

Here, P_1 is the probability of foEs exceeding the frequency f_1, with an analogous meaning for P_2. b is a negative constant which is a function of location. A value of -0.23 for b is a reasonable approximation for most locations (Phillips, 1963). Hence, from available world maps of the probability of foEs exceeding 7 MHz (Smith, 1976), it is possible to calculate the probability that foEs sec(ϕ) will exceed fob. Phillips (1963) recommends that the probability distribution sought should not be that of foEs being less than $f\nu$, but of fbEs being less than $f\nu$, since such layers are totally reflecting. In this case, foEs must be exceed some frequency which is larger than $f\nu$; consequently, the probability P will be smaller. Phillips (1963) recommends using a frequency of $f\nu/0.7$ for nighttime propagation and a value of $f\nu/0.9$ for daytime propagation.

Lloyd et al. (1978) suggest that the probability distribution of foEs about its average value is roughly Gaussian. Hence, the probability P is given by

$$P = \frac{1}{\sqrt{2\pi}} \int_z^\infty e^{-\frac{1}{2}\alpha^2} \, dx \tag{83}$$

$$Z = \frac{fob - \overline{foEs}\ sec(\phi)}{\sigma\ sec(\phi)} \ , \tag{83a}$$

where $\overline{foEs}$ is the average value of foEs, and σ is the variance of foEs about its mean. Similarly, the power loss (in decibels) due to transmittance through the sporadic E layer is given by 10 log(1-P) (Phillips, 1963). The value of σ can be determined from the fact that for a Gaussian distribution

with zero mean, the value which is exceeded 90% of the time is 1.28 σ below the mean. Using these values for the reflection and transmission losses, it is possible, by tracing rays through the ionosphere, to determine the effects of the sporadic E layers on the signal strength.

For frequencies above the MUF, the signal does not fall abruptly to zero, as would be expected on the basis of geometrical optics. Signals can be scattered from the D, E, and F regions into the skip zone. The Phillips-Abel theory can be used to describe the effects of this process (Phillips, 1963, Wheeler, 1966). The procedure is similar to that employed in describing the sporadic E signal. Instead of envisioning the E layer as composed of regions corresponding to a distribution of foEs values, the ionosphere is now considered to be composed of regions associated with a distribution of MUF values. When the frequency f is less than a particular MUF value, the wave will not be reflected into the skip zone. In this view, rays can be reflected, just as they are for frequencies below the MUF, from the ionosphere to the receiver. The power reflected is proportional to the probability P that the frequency f is less than the MUF. There are no obscuration losses for frequencies above the MUF, since there are no reflections from the normal F layer.

The distribution of MUF values is roughly Gaussian (Phillips, 1963, Wheeler, 1966); hence, P can be calculated. The actual ray path of the reflected wave can be assumed to be identical to the path associated with the MUF (CCIR, 1984). In this way the absorption loss L_i can also be calculated.

IONCAP (Lloyd et al., 1978) calculates the over-the-MUF loss at all frequencies in order to incorporate the possibility that the MUF will be below the average MUF. The CCIR model (CCIR, 1984) uses an approximate form for the

over-the-MUF loss L_M, which is only used for frequencies above the MUF; namely,

$$L_M \quad 130\left(1 - \frac{f}{MUF}\right)^2 \quad . \tag{84}$$

Damboldt and Sussman (1976) have proposed a very simple method for calculating the over-the-MUF loss. The model is intended to be simply appended to any model that is acceptable for frequencies below the MUF and is expected to be adequate for ranges less than about 3000 km. The field above the MUF expressed in decibels above 1 μV/m, F, is fit to the following functional form

$$F = ae^{-bf} + c \ , \tag{85}$$

where a, b, c are constants and f is the frequency.

The operational MUF is defined by Damboldt (1976) as that frequency f_m at which a transmitter with 1000 kW effective radiated power will produce a field at the receiver of 1 μV/m. Empirically it is found that f_m is given approximately by

$$f_m = 2.5\left(\frac{f_{min}}{f_{max}}\right)^{.7} (MUF) \ , \tag{86}$$

where f_{min} denotes the larger of foE or foF2 at noon; and f_{max} denotes the larger of foE or foF2 at the particular hour desired (Damboldt and Sussman, 1976).

Damboldt and Sussman (1976) assume that c has a value of -50. This choice must be dependent upon the manner in which their data was derived. Their data were collected with a transmitter operating at 1 kW effective radiated power. If the field produced by a given transmitter is expressed relative to the field produced by their experimental setup, then we have that

$$F = F_{DS} + 10 \log(P) + 10 \log(G_T) - 4.8 \ , \tag{87}$$

where F_{DS} is the field, expressed in dB above 1 μV/m, produced by Danbolt and Sussman's transmitter; F is the field, expressed in decibels above 1 μV/m, of an arbitrary transmitter; P is the power relative to 1 kW; and G_T is the gain relative to an isotropic radiator. F_{DS} is equal to equation (85), with c equal to -50. By matching equation (87) to the values of the fields at the MUF and f_m, we obtain

$$a = 20 \text{ X } 10^{0.434bf_m} \tag{88}$$

$$b = \frac{\log\left[F_M - 10 \log(P) - 10 \log(G_T) + 54.8\right] - \log(20)}{0.434(f_m - MUF)} \tag{89}$$

$$F = 20e^{-b(f-f_m)} + 10 \log(P) + 10 \log(G_T) - 54.8 \ , \tag{90}$$

where F_M is the field expressed in decibels above 1 μV/m at the MUF. F_M is obtained from whatever model is used below the MUF. It should be noted that Damboldt and Sussman (1976) caution the user of this model that it has not been adequately tested. In fact, the Deutsche Bundespost, for which the above model was designed, is presently using a different short range-model (Bradley and Liu, 1982).

We can now derive an expression for the magnitude of the field strength E at the receiver. We have

$$20 \log(E) = 104.8 + 10 \log(P) - 20 \log(D') + 10 \log(G_T) - L_B \ , \tag{91}$$

where E is expressed in microvolts per meter, P is expressed in kilowatts, D' is the virtual slant range of the ray expressed in kilometers, G_T is the gain of the transmitter relative to an isotropic radiator, and L_B represents the additional losses. The virtual slant range D' is an approximation to the group path. The virtual slant range is the distance which a ray in free space

would travel in going from the receiver to the transmitter via one or more reflections at the virtual height of reflection. Generally, due to absorption in the D layer, no more than two E layer hops are considered. In addition to reflections from either the F or E layers, the possibility of mixed modes should also be considered. For example, a mode which only passes through the D layer twice would be one which reflects from the F layer, the topside of a sporadic E layer, and the F layer. Generally, the field strength is determined by considering only that mode which produces the smallest loss (CCIR Report 252-2, 1970, Lucas and Haydon, 1966, Laitinen and Haydon, 1962, Lloyd et al., 1978). This is an incorrect procedure for ranges greater than about 10,000 km (Lloyd et al., 1978) and is probably not an acceptable procedure for ranges greater than 7000 km.

L_B in equation (91) is given by

$$L_B = L_G + L_M + L_o + L_r + l_i \ , \tag{92}$$

where L_G are the losses due to reflection from the ground, L_M the F layer over-the-MUF losses, L_o the obscuration losses, L_r the losses due to reflection from sporadic E layers, and L_i the absorption losses. For frequencies above the MUF, $(L_o + L_r)$ can be replaced by Γ as given by Miya et al. (1978) or by the CCIR model (CCIR Recommendation 534, 1978 or CCIR Recommendation 534-1, 1982). The 1984 CCIR model (CCIR, 1984) for field strength does not explicitly include the effects of sporadic E propagation. Instead, it replaces Y_p of equation (79) with a new set of correction factors, which are a function of season and location. The 1970 CCIR model (CCIR Report 252-2, 1970) does not include an over-the-MUF loss, since it was not intended to be used for frequencies greater than the MUF.

For ranges less than about 7000 km, the field strength is dominated by a single mode of propagation. Except for the ducted mode, equation (91) is applicable for all of these modes. Hence, in order to determine the dominant mode, the largest field strength calculated on the basis of equation (91) must be compared with ducted field strength. The 1984 CCIR model (CCIR, 1984) adds together, on an incoherent basis, the three strongest modes. This can also be done here, the only difference being that now an additional mode, heretofore unaccounted for (the ducted mode), is to be included in the set of possible modes.

As the range increases, the number of modes which contribute significantly to the received signal strength increases, and as the number of independent signals increases, the resulting interference pattern begins to take on the characteristics of a random field. Consequently, for ranges greater than about 9000 km, the calculation of the field strength becomes essentially statistical and the resolution of the individual components of little value. For these ranges a new method of field strength calculation is needed. We will discuss two models: the Deutsche Bundespost model and the IONCAP model.

The Deutsche Bundespost model (Damboldt, 1976) is an empirical model that was designed primarily to deal with propagation at frequencies greater than the MUF and for ranges greater than 4000 km (Beckmann, 1965). It takes into account all modes of propagation above the MUF, but makes no attempt to distinguish between the effects of any particular mode. The formulation of this model begins with the observation that the signal received as a function of frequency rises from the lowest usable frequency (LUF) to a maximum and then declines to the upper receiving limit (MUF) (Beckmann, 1965). The MUF

usually lies somewhat above (by 10% to 20% or even more) the frequency associated with the maximum of the received field strength (Beckmann, 1965).

For signal strengths below the maximum value, the daytime signal strength decreases as the frequency decreases. This result can be understood as follows. Near the LUF, the losses associated with the particular mode of propagation must be near their minimum values. If this were not the case, there would exist modes of propagation with less loss. Hence, the frequency could be decreased and still sustain the same or less loss. Thus, near the LUF there exists, generally, only a single mode of propagation; and that mode of propagation is the mode associated with the smallest losses at that frequency. The mode with the smallest losses is one which has the smallest number of ground reflections and passages through the D layer and smallest free space loss. Clearly, the mode associated with the smallest losses will, therefore, be associated with the ray trajectory that possesses the smallest number of hops and the smallest elevation angle. Because deviative absorption is generally most important near the peak of the layer, the major portion of the absorption losses for this ray trajectory will be due to nondeviative absorption. Ground losses are generally negligible compared with the absorption losses; hence, the loss near the LUF is primarily due to the sum of the nondeviative absorption loss and free space loss.

The expression used by the Deutsche Bundespost to describe the nondeviative absorption loss L is modeled after equation (78). It is of the form

$$L = \frac{B_0 \sec(\phi) M}{(f + f_H)^2}, \tag{93}$$

where B_0 is a constant; M is a function of season, geographical location, and solar zenith angle; and all other quantities have the same meaning as in equation (79). The expression for M is given by the Deutsche Bundespost (Damboldt, 1976) as

$$M = \sum_{j=1}^{2n} J_j[\cos(\chi_j)]^{1/2}(1 + 0.005R_{12}) , \tag{94}$$

where J_j is a function of season and the geographical location of both terminals, and all other quantities have the same meaning as in equation (79). Each term in the sum is determined twice for each of n hops, once for each passage through the D layer.

So, for frequencies near the LUF, the field strength E expressed in decibels above 1 μV/m is approximately given by

$$20 \log(E) = Edb = E_0 + 10 \log(P) + 10 \log(G_T) - L , \tag{95}$$

where the free space field strength E_0 expressed in decibels above 1 μV/m is given by

$$E_0 = 104.8 - 20 \log(D') . \tag{96}$$

Here, all quantities have the same meaning as in equation (91).

The Deutsche Bundespost model defines the LUF as that frequency which produces a field of 1 μV/m at the receiver with a transmitter of 1000 kW effective radiated power (Damboldt, 1976). The effective radiated power corresponds to an isotropic radiator with a gain of 4.8 dBI (i.e., relative to an isotropic radiator in free space). Using this definition in equation (96), we obtain

$$LUF = \left(\frac{B_0 \sec(\phi)M}{E_0 + 34.8}\right)^{1/2} - f_H . \tag{97}$$

Here, we have used equation (93) for L. The CCIR version of this model multiplies this expression by a winter-anomaly factor A_w; otherwise it is identical to the Deutsche Bundespost model (CCIR, 1984). The CCIR (CCIR, 1984) provides tables of values for the quantities B_0 and M. The virtual slant range D' is determined by assuming a virtual reflection height of 300 km, and the gain G_T is the maximum value of the gain in the range of 8 to 10 deg above the horizontal (CCIR, 1984).

Letting

$$f_z = f + f_H \text{ and } f_L = LUF + f_H \tag{98}$$

in equation (97), we have that the field strength well below the MUF is approximately given by

$$Edb = [e_0 = 34.8]\left[1 - \left(\frac{f_L}{f_z}\right)^2\right] + \langle 10 \log(P) + 10 \log(G_T) - 34.8\rangle \ . \tag{99}$$

If the transmitter has an effective radiated power of 1000 kW, the expression enclosed by the angle brackets is zero. The resulting expression is the result obtained by Beckmann (1965).

As the frequency increases above the MUF, the losses increase with frequency (Beckmann, 1965). Define the "operational MUF" as that frequency at which the field decreases to a value of 1 μV/m for a transmitter of 1000 kW of effective radiated power (Beckmann, 1965, Damboldt, 1976). The functional form of the field strength, in decibels, above its maximum implies that the loss is proportional to f_z^2. Adding this term to equation (99) and requiring that Edb is zero both at the LUF and the "operational MUF," fm, for a transmitter of 1000 kW effective radiated power, we obtain

$$EdB = [e_0 = 34.8]\left\{1 - R\left[\left(\frac{f_L}{f_z}\right)^2 + \left(\frac{f_z}{f_v}\right)^2\right]\right\}$$

$$+ [10 \log(P) + 10 \log(G_T) - 34.8] , \qquad (100)$$

where

$$R = \frac{fv^2}{f_L^2 + fv^2} \qquad (101)$$

and

$$fv = f_m + f_H . \qquad (102)$$

The value of f_m is determined from (Beckmann, 1965, Damboldt, 1976, CCIR, 1984):

$$f_m = K(MUF) , \qquad (103)$$

where MUF is the median standard MUF. K is a constant which depends on the location of the transmitter and the time and direction of propagation. K is a function of various coefficients, whose values are constantly being readjusted as more experimental data become available (CCIR, 1984). Values for K are given by the CCIR (CCIR, 1984) and Damboldt (1976).

It is worth noting that although the frequencies LUF and f_m are referred to as the lowest usable frequency and operational frequency, respectively, they are not defined in the way that is typical of these frequencies. In fact, we have explicitly tried to distinguish the MOF from the operational frequency. The LUF and operational MUF are generally functions of the transmitter output and receiver sensitivity. However, the LUF and operational MUF as used by Beckmann (1965) are simply two frequencies at which the field strength is determined. Because the field strength measured in decibels, EdB, is a relatively simple function of frequency f, these two points are sufficient to approximately define the functional relationship between EdB and f.

Equation (100) for EdB is the basic form used by both the Deutsche Bundespost (Damboldt, 1976) and the CCIR (CCIR, 1976) models. The CCIR model includes additional terms to account for focusing at long ranges and a correction term to adjust the result to agree with recent empirical data (CCIR, 1984). Both models use a different expression for f_L during the nighttime and for periods of transition between night and day (CCIR, 1984, Damboldt, 1976). The expressions used are similar. The Deutsche Bundespost uses this model for ranges greater than 4000 km, whereas the CCIR model reserves its use for ranges greater than 9000 km.

The model used by IONCAP is considerably more physical than the empirical model just discussed. Lloyd et al. (1978) view the propagation mode for long ranges as due to the coupling of energy, via scattering, into propagation modes otherwise unavailable. They suggest that the most favorable mode would be one which by a series of reflections between the F layer and the top of sporadic E layers reaches the receiver with the fewest passages through the D layer. Reflection losses at sporadic E layers and ground losses are calculated for the principal path. The absorption loss L_i is modified for these long paths and a convergence factor is added (Lloyd et al., 1978). With the available documentation, it is difficult to be more explicit.

4.4 SUMMARY FOR RANGES GREATER THAN 500 km

The types of models available can be divided into three classifications: (i) those that deal with frequencies below the MUF and moderate ranges, (ii) those that deal with frequencies greater than the MUF and moderate ranges, and (iii) those that deal with long-range propagation. Of course, some models deal with all these possibilities.

Below the MUF, the most complicated and thorough model is IONCAP. The model that is simplest to apply is the 1984 CCIR model (CCIR, 1984). The 1970 CCIR model possesses a degree of complexity and thoroughness that lies somewhere between these two models (CCIR Report 252-2, 1970).

The effect of sporadic E for frequencies below the MUF is probably more accurately handled by the method given by Sinno et al. (1976) than the Phillips-Abel method (Phillips, 1963, Lloyd et al., 1978). Both methods require information which may not be easily obtained. The method of Sinno et al. (1976) requires knowledge of the blanketing frequency fbEs. Statistics on fbEs are not as widely available as those for foEs (Phillips, 1963). The method used by IONCAP requires knowledge of the variance of foEs. This information could be obtained from the data available on foEs, albeit at the expense of much computer time. For frequencies above the MUF, the method proposed by Miya et al. (1978) is, at present, the best available method of calculating the sporadic E signal strength. With only minor modifications this is the method recommended by the CCIR in 1978 and 1982 (CCIR Recommendation 534, 1978, CCIR Recommendation 534-1, 1982). The 1982 version has been simplified relative to the 1978 version.

The over-the-MUF loss used by the 1984 CCIR model is so simple as to lead one to doubt its usefulness. The model proposed by Damboldt and Sussman (1976), though untested, may prove to be an adequate yet sufficiently simple model to be easily employed. However, the simplicity of this model is somewhat misleading, since the computer time spent in determining f_{min} and f_{max} may be considerable. Since this empirical model attempts to account for all over-the-MUF losses, it should not be used with any other over-the-MUF model (e.g., a sporadic E model). The advantage of the methods used by IONCAP is that the effects of the E and F layers can be accounted for separately.

The two models discussed for long-range propagation are the Deutsche Bundespost model and IONCAP. It is difficult to assess the advantages of one over the other. The Deutsche Bundespost model has been tested and shown to give adequate results (Damboldt, 1976). Greater use of this model will undoubtedly improve its performance. We could find no information on the adequacy of the method employed by IONCAP.

One area in which all models are deficient is in the calculation of auroral absorption losses. It is hoped that future research will remedy this deficiency. However, in all other respects, adequate methods for calculating the field strength in the LoVHF band already exist.

BIBLIOGRAPHY

Al'pert, Y. L., Radio Wave Propagation and the Ionosphere, Volume 1, The Ionosphere, Consultants Bureau, 1973.

Appleton, E.V., and W.J.G. Beynon, The application of ionospheric data to radio-communications problem: part I, Proc. Phys. Soc., 52, 518-533, 1940.

Appleton, E.V., and W.J.G. Beynon, The application of ionospheric data to radio-communication problems: Part II, Proc. Phys. Soc., 59, 58-76, 1947.

Bailey, D.K., R. Bateman, and R.C. Kirby, Radio transmission at VHF by scattering and other processes in the lower ionosphere, Proc. IRE., 43, 1181-1230, 1955.

Bateman, R., J.W. Finney, E.K. Smith, L.H. Tveten, and J.M. Watts, IGY observations of F-layer scatter in the Far East, J. Geo. Res., 64, 403-405, 1959.

Baumgartner, G.B., H.V. Hitney, R.A. Pappert, Duct propagation modelling for the Integrated Refractive-Effects Prediction System (IREPS), IEE Proc., 130, part F, 630-642, 1983.

Baumgartner, G.B., XWVG: a waveguide program for trilinear tropospheric ducts, NOSC Techical Document 610, Naval Ocean Systems Center, San Diego, CA 92152, 1983.

Bean, B.R., and E.J. Dutton, Radio Meteorology, National Bureau of Standards Monograph 92, 1966.

Beckmann, B., Notes on the relationship between the receiving-end field strength and the limits of the transmission frequency range MUF, LUF, NTZ, 19, 643-653, 1965.

Bibl, K., K. Rawer, and E. Theissen, An improved method for the calculation of the field strength of waves reflected by the ionosphere, Nature, 169,147-148, 1952.

Booker, H.G., and W. Walkinshaw, The mode theory of tropospheric refraction and its relation to wave-guides and diffraction, in Meteorological Factors in Radio Wave Propagation, London, Physical Soc., 80-127, 1946.

Booker, H.G., and W.E. Gordon, A theory of radio scattering in the troposphere, Proc. I.R.E., 38, 401, 1950.

Booker, H.G., and J.T. DeBettencourt, Theory of radio transmission by tropospheric scattering using very narrow beams, Proc. IRE., 43, 281-290, 1955.

Bradley, P.A., and R.Y. Liu, An evaluation of the FTZ HF sky-wave field-strength prediction method, CCIR XVIth Plenary Assembly, Study Group 6, Interim Working Parties 6/1 and 6/12, 1982.

Budden, K.G., The Wave-guide Mode Theory of Wave Propagation, Prentice-Hall Inc., 1961a.

Budden, K.G., Radio Waves in the Ionosphere, Cambridge Univ. Press, 1961b.

Bullington, Kenneth, Radio propagation at frequencies above 30 megacycles, Proc. IRE., 35, 1122-1136, 1947.

Burrows, C.R., and M.C. Gray, The effect of the earth's curvature on ground-wave propagation, Proc. I.R.E., 29, 16-24, 1941.

Burrrows, W.G., VHF Radio Wave Propagation in the Troposphere, Intertext Books, 1968.

CCIR, CCIR atlas of ionospheric characteristics, Report 340, Oslo, 1966, International Radio Consultative Committee, International Telecommunication Union, Geneva, 1967.

CCIR, CCIR interim method for estimating sky-wave field strength and transmission loss at frequencies between the approximate limits of 2 and 30 MHz, Report 252-2, New Delhi, 1970, International Radio Consultative Committee, International Telecommunication Union, Geneva, 1970.

CCIR, Recommendations and reports of the CCIR, 1978, XIVth Plenary Assembly, Kyoto, 1978, Vol. VI, Propagation in ionized media, Report 259-4, International Radio Consultative Committee, International Telecommunication Union, Geneva, 1978.

CCIR, Recommendations and reports of the CCIR, 1978, XIVth Plenary Assembly, Kyoto, 1978, Vol. VI, Propagation in ionized media, Recommendation 534, International Radio Consultative Committee, International Telecommunication Union, Geneva, 1978.

CCIR, Recommendations and reports of the CCIR, 1982, XVth Plenary Assembly, Geneva, 1982, Vol. VI, Propagation in ionized media, Recommendation 534-1, International Radio Consultative Committee, International Telecommunication Union, Geneva, 1982.

CCIR, Report to the second session of the conference, World Administrative Radio Conference for the planning of the HF bands allocated for the broadcasting service, First Session, Geneva, 1984, Annex 1, General Secretariat of the International Telecommunication Union, Geneva, 1984.

Cohen, R., and K. L. Bowles, On the nature of equatorial spread F, J. Geo. Res., 66, 1081-1106, 1961.

Cracknell, R.G., Twenty-one years of TE, Radio Communication, 56, 785-788, Aug. 1980.

Damboldt, T., and P. Sussman, Extending field-strength predictions (for short distances) to frequencies above the standard MUF, CCIR XIVth Plenary Assembly, Study Group 6, Interim Working Party 6/1, Doc. 45, 1976.

Davies, K., Ionospheric Radio Propagation, National Bureau of Standards Monograph 80, 1965.

Davies, K., Ionospheric Radio Waves, Blaisdell Pub. Co., 1969.

Dolukhanov, M., Propagation of Radio Waves, Mir Pub., 1971.

Ferguson, J.A., and H.G. Booker, A scattering theory of VHF transequatorial propagation, J. Atmos. Terr. Phys., 45, 641-647, 1983.

Ferguson, J.A., Application of a scattering theory of VHF transequatorial propagation, J. Atmos. Terr. Phys.,46, 643-661, 1984.

Fishback, W.T., Methods for calculating field strength with standard refraction, in Propagation of Short Radio Waves, ed. D.E. Kerr, Boston Technical Pub., Inc., 1964.

Frank, V. R., Propagation predictions for May, Ham Radio, 2, 61-67, May 1969.

Freehafer, J.E., Chapter 2, in Propagation of Short Radio Waves, ed. D.E. Kerr, Boston Technical Pub., Inc., 1964.

Hagn, G.H., B.M. Sifford, and R.A. Shepherd, The SRICOM probabalistic model of communication system performance, SRI project 3603, SRI International, 1611 North Kent Street, Arlington, VA 22209, 1982.

Hall, M.P.M., Effects of the Troposphere on Radio Communication, Peter Peregrinus Ltd., 1979.

Heron, M.L., Recent progress in transequatorial propagation-review, J. Atmos. Terr. Phys., 43, 597-606, 1981.

Hitney, H.V., C.P. Hattan, R.A. Paulus, and K.D. Anderson, Electromagnetic propagation function program performance specification (PPS) for the tactical environmental support system (TESS), NOSC Technical Note 1325, Naval Ocean Systems Center, San Diego, CA 92152, 1984.

Hitney, H. V., J. H. Richter, R. A. Pappert, K. D. Anderson and G. B. Baumgartner, Jr., Tropospheric radio propagation assessment, Proc. IEEE., 73, 265-283, 1985.

IEEE. Spectrum, 20, May 1985, Whatever happened to meteor-burst communications?

Jacobs, G., and S. Leinwoll, VHF ionospheric propagation, CQ, 25, 37-42, Nov. 1969.

Jacobs, G., and T. J. Cohen, The Shortwave Propagation Handbook, Cowan Pub. Co., 1979.

Jones, H.E.R., Communications in the skip-zone using backscattering from ionized meteor trails and E-layer turbulences, in Effect of the Ionosphere on Radiowave Systems, ed. by John M. Goodman, jointly sponsored by the Naval Res. Lab., Office of Naval Res., and the Air Force Geo. Lab., 325-338, 1981.

Kerr, D.E ., Theory of Specular Reflections, in Propagation of Short Radio Waves, ed. D.E. Kerr, Boston Technical Pub., Inc., 1964.

Kift, F., The propagation of high-frequency radio waves to long distances, Proc. IEE, 107B, 127-140, 1960.

Kneisel, T. F., Ionospheric scatter by field-aligned irregularities at 144 MHz, QST, 66, 30-32, Jan. 1982.

Kobayashi, T., Transmission curves for the curved ionosphere, J. Radio Res. Labs, Tokyo, 8, 395-411, 1961.

Kovalevskaya, YE. M., and Ye. A. Kornitskaya, Influence of the horizontal gradients of the parameters of electron density distribution on the MUF, hop distance, and angles of arrival, Geomagnetism and Aeronomy, 9, 232-234, 1969.

Laitinen, P.O., and G.W. Haydon, Analysis and prediction of sky-wave field intensities in the high frequency band, Tech. Report No. 9., U.S. Army Signal Radio Propagation Agency, Fort Monmouth, NJ 1962.

Lange-Hesse, G., VHF bistatic auroral backscatter communication, in Ionospheric Radio Communications, ed. by K. Folkestad, 1968.

Leftin, M., Numerical representation of monthly median critical frequencies of the regular E region (foE), OT Report 76-88, Boulder, CO, 1976.

Lloyd, J.L., G.W. Haydon, D.L. Lucas, and L.R. Teters, Estimating the performance of telecommunication systems using the ionospheric transmission channel, Vol. I, Institute for Telecommunication Sciences, Boulder, CO 80303, (unpublished report), 1978.

Lockwood, M., Simple M-factor algorithm for improved estimation of the basic maximum useable frequency of radio waves reflected from the ionospheric F-region, IEE proc., 130, 296-302, 1983.

Longley, A.G., and P.L. Rice, Prediction of tropospheric radio transmission loss over irregular terrain, ESSA Tech. Report ERL 79-ITS 67, Institute for Telecommunication Sciences, Boulder, CO 80303, 1968.

Lucas, D.L., and G.W. Haydon, Predicting statistical performance indexes for high frequency telecommunications systems, ESSA Tech. Report IER 1-ITSA 1, Institute for Telecommunication Sciences and Aeronomy, 1966.

Lustgarten, M.N., An empirical propgagation model (EPM-73), IEEE. Trans. EC., EMC-19, 301-309, 1977.

Matthews, P.A., Radio Wave Propagation VHF and Above, Chapman and Hall Ltd., 1965.

Miya, K., and T. Sasaki, Characteristics of ionospheric Es propagation and calculation of Es signal strength, Radio Sci., 1, 99-108, 1966.

Miya, K., K. Shimizu and T. Kojima, Oblique-incidence sporadic-E propagation and its ionospheric attentuation, Radio Sci., 13, 559-570, 1978.

Nielson, D.L., Oblique sounding of a transequatorial path, in Spread F and its Effects upon Radiowave Propagation and Communication, ed. P. Newman, Technivision, Maidenhead, England, 1966.

Nielson, D.L., Long-range VHF Propagation Across the Geomagnetic Equator, Stanford Res. Inst., 1969.

Norton, K.A., The calculation of ground-wave field intensity over a finitely conducting spherical earth, Proc. I.R.E., 29, 623-639, 1941.

Pappert, R.A., and C.L. Goodhart, Case studies of beyond-the-horizon propagation in tropospheric ducting environments, Radio Sci., 12, 75-87, 1977.

Pappert, R.A., and C.L. Goodhart, A numerical study of tropospheric ducting at HF, Radio Sci., 14, 803-813, 1979.

AD-A169 332 PROPAGATION OF SIGNALS IN THE FREQUENCY BAND BETWEEN 30 MHZ AND 100 MHZ(U) NAVAL OCEAN SYSTEMS CENTER SAN DIEGO CA W POWERS ET AL. SEP 85 NOSC/TR-1087 2/2

UNCLASSIFIED F/G 20/14 NL

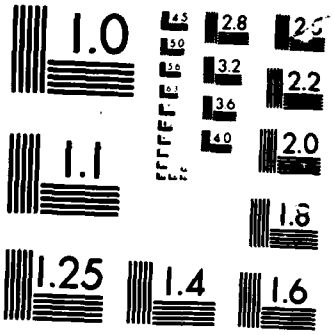

MICROCOPY CHART

Patterson, W.L., Climatology of Marine Atmospheric Refractive Effects, NOSC Technical Document 573, Naval Ocean Systems Center, San Diego, CA 92152, 1982.

Phillips, M.L., Auxiliary procedures used in theoretical evaluation of H-F backscatter observations and other communications problems, External Tech. Memo No.14, Electro-Physics Labs, 1963.

Rastogi, R.G., and R.F. Woodman, VHF radio wave scattering due to range and frequency types of equatorial spread-F, J. Atmos. Terr. Phys., 40, 485-491, 1978.

Reed, H. R., and C. M. Russell, Ultra High Frequency Propagation, Boston Technical Pub., Inc., 1964.

Roberts, W. M., and R. K. Rosich, Maximum Usable Frequencies MUF (Zero)F2, KMUF(4000)F2, MUF(2000)E for a Maximum Solar Activity Period of an Average Solar Cycle, R12=10, U.S. Dept. of Commerce, Office of Telecommunications, Inst. for Telecommunication Sciences, 1971a.

Roberts, W. M., and R. K. Rosich, Maximum Usable Frequencies MUF (Zero)F2, MUF(4000)F2, MUF(2000)E for a Maximum Solar Activity Period of an Average Solar Cycle, R12=110, U.S. Dept. of Commerce, Office of Telecommunications, Inst. for Telecommunication Sciences, 1971b.

Rose, R.B., J.N. Martin, and P.H. Levine, Minimuf-3: a simplified HF MUF prediction algorithm, NOSC Tech. Report 186, Naval Ocean Systems Center, San Diego, CA 92152, 1978.

Rosich, R.K., and W.B. Jones, The numerical representation of the critical frequency of the F1 region of the ionosphere, OT Report 73-22, Boulder, CO, 1973.

Sailors, D.B., W.K. Moision and T.N. Roy, The New U.S. Army PROPHET Evaluation System (APES) Models, NOSC Technical Document 642, Naval Ocean Systems Center, San Diego, CA 92152, 1983.

Schwartz, M., W.R. Bennett, and S. Stein, Communication Systems and Techniques, McGraw-Hill Book. Co., 1966.

Shimazaki, T., Worldwide daily variations in the height of the maximum electron density of the ionospheric F2 layer, J. Radio Res. Labs., Tokyo, Japan, 2, No. 7, 86-97, 1955.

Sinno, K., Kan, M., and Y. Hirukawa, On the reflection and transmission losses for ionospheric radio wave propagation via sporadic E, J. Radio Res. Lab., Tokyo, 23, 65-84, 1976.

Smith, E. K., World maps of sporadic E (foEs > 7 MHz) for use in prediction of VHF oblique-incidence propagation, U.S. Dept of Commerce, OT special publication 76-10, 1976.

Smith, N., The relation of radio sky-wave transmission to ionosphere measurements, Proc. I.R.E., 27, 332-347, 1939.

Stein, S., and J.J. Jones, Modern Communication Principles, McGraw-Hill Book Co., 1967.

Stewart, J., Sporadic E on 144 MHz - 1983, QST, 68, 23-24, Feb. 1984.

Sugar, G. R., Radio propagation by reflection from meteor trails, Proc. IEEE., 116-136, 1964.

Tilton, E. P., The Radio Amateur's VHF Manual, Amer. Radio Relay League, Inc., 1968.

Vergara, W.C., J.L. Levatich and T.J. Carroll, VHF air-ground propagation far beyond the horizon and tropospheric stability, IRE Trans. AP, 608-621, 1962.

Wheeler, J.L., Transmission loss for ionospheric propagation above the standard MUF, Radio Sci., 1, 1301-1308, 1966.

Wheelon, A. D., Radio-wave scattering by tropospheric irregularities, J. Res. NBS., 63D, 205-233, 1959.

END

DTIC

7-86